rather than the regulatory subunit PP2A-B56 (Supplementary Figs 1 and 6). Curiously, when centromeric PP2A was displaced by *hSgo2* siRNA, hSgo1 localization was not impaired, although it was reduced by the depletion of PP2A (Fig. 3a). This may indicate that hSgo1 dynamically associates with centromeres, and that cytoplasmic PP2A may influence this interaction. If either hSgo1 or centromeric PP2A (using *hSgo2* siRNA) is absent from the centromere, the protection of sister centromeres is impaired, suggesting that both proteins collaboratively function at the centromere to protect the dissociation of cohesin.

The shugoshin complex counteracts phosphorylation of SA

Given that phosphorylation of the cohesin subunit SA2 (and presumably SA1) by Plk1 is critical for cohesin dissociation[17], we proposed that SA2 phosphorylation is counteracted by the shugoshin–PP2A complex at centromeres. To examine whether cohesin SA2 preserved around centromeres is indeed dephosphorylated *in vivo*, we prepared nocodazole-treated prometaphase cells in which cohesin is largely dissociated from the chromosome arms but tethered exclusively at centromeres, depending on shugoshin and PP2A (Fig. 2f). The cell extracts were fractionated into chromatin-bound and -unbound fractions, separated by SDS–polyacrylamide gel electrophoresis (SDS–PAGE), and blotted with anti-SA2 antibodies. As expected, SA2 showed slow electrophoretic migration in the prometaphase chromatin-unbound fraction, representing phosphorylation (presumably by Plk1)[17]. In contrast, chromatin-bound SA2 was mostly dephosphorylated (Fig. 4a). These results suggest that SA2 preserved at centromeres is dephosphorylated *in vivo*.

We next examined the biochemical properties of the shugoshin complex *in vitro*. We prepared a carboxy-terminal peptide of SA2 (SA2-C), in which most of the phosphorylation sites are included[17], and phosphorylated it with recombinant Plk1 *in vitro*. The phospho-labelled SA2 fragment was then mixed with purified hSgo1 complex. The results show that immunoprecipitates of hSgo1 can dephosphorylate SA2-C, and that this phosphatase activity is inhibitable by okadaic acid (Fig. 4b). Similar phosphatase activity was detected in the hSgo2 immunoprecipitates. These phosphatase activities also dephosphorylated a C-terminal peptide of SA1 that had been phosphorylated by Plk1, but not histone H3 phosphorylated by Aurora B kinase, indicative of substrate specificity. Thus, the shugoshin complex has the ability to counteract the phosphorylation of Scc3/SA *in vitro*. Taken together, these results support the hypothesis that PP2A-dependent dephosphorylation of Scc3/SA prevents the dissociation of cohesin from centromeres, as part of the centromeric protection function of the shugoshin complex.

PP2A is required for centromeric protection in meiosis

Schizosaccharomyces pombe Sgo1 protects centromeric cohesin containing Rec8 from separase cleavage at meiosis I[8,9]. In a yeast two-hybrid screen searching for proteins that interact with Sgo1, we frequently isolated Par1—one of the PP2A-B56 homologues in fission yeast[28]. The interaction between Sgo1 and Par1 was confirmed by immunoprecipitation (Fig. 5a). In proliferating cells, Par1 localizes in the cytoplasm, and on the spindle pole body and the division septum (data not shown)[28,29]; however, it colocalizes with Sgo1 at centromeres during meiosis I (Fig. 5b). Sgo1 localization was not impaired in mutant *par1Δ* cells (data not shown). In contrast, the centromeric localization of Par1 was abolished in mutant *sgo1Δ* cells (Fig. 5c), indicative of the dependency of Par1 localization on shugoshin and reminiscent of the situation in human mitotic cells.

To examine whether Par1 is required for the protection of centromeric cohesin during meiosis, we analysed Rec8 localization at metaphase II—the period during which Rec8 is detected only at centromeres. We found that, like *sgo1Δ* cells, *par1Δ* cells mostly lost

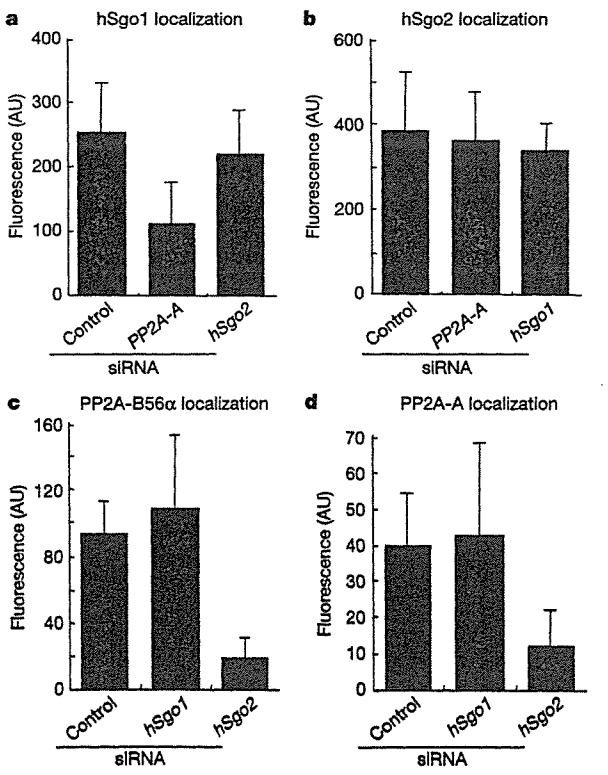

Figure 3 | Interdependency of shugoshin and PP2A for localization. **a–d**, Cells after siRNA treatment were stained with the indicated antibodies (**a**, hSgo1; **b**, hSgo2; **c**, PP2A-B56; **d**, PP2A-A; see also the representative stained cells in Supplementary Fig. 4). The intensities of the fluorescent centromeric signals in prometaphase cells were quantified as described in Methods. AU, arbitrary units. Error bars represent s.d. ($n = 20$).

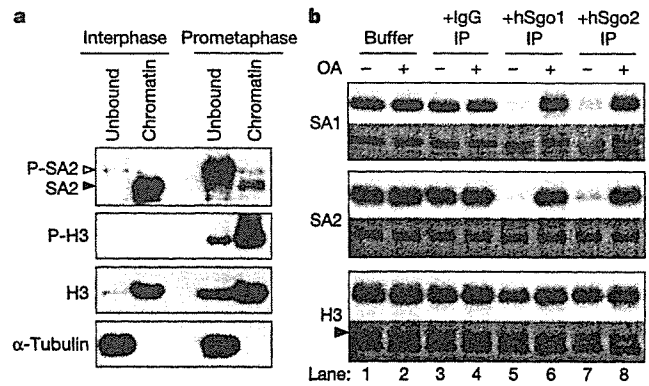

Figure 4 | Dephosphorylation of cohesin subunit SA. **a**, Chromatin-bound SA2 is dephosphorylated *in vivo*. Cell extracts prepared from interphase and prometaphase cells were fractionated into chromatin-bound and -unbound fractions and analysed by western blotting with the indicated antibodies. Four-times more of the chromatin-bound fractions were loaded. P-SA2, phosphorylated SA2; P-H3, histone H3 phosphorylated on Ser 10. In the mitotic chromatin-bound fraction, contaminated interphase chromatin is, if any, negligible (see Supplementary Fig. 9). **b**, Endogenous shugoshin associates with an okadaic-acid-inhibitable phosphatase activity that dephosphorylates cohesin subunit Scc3/SA. C-terminal peptides of SA1 or SA2 phosphorylated by Plk1, and a control histone H3 phosphorylated by Aurora B, were mixed with immunoprecipitation (IP) buffer (lane 1 and 2), control IgG immunoprecipitates (lane 3 and 4), immunoaffinity-purified hSgo1 (lane 5 and 6) or hSgo2 (lane 7 and 8) from HeLa cell extracts. Each sample was incubated in the presence (+) or absence (−) of 1 μM okadaic acid (OA) for 2 h. Autoradiography is shown in the upper panel, Coomassie blue staining in the lower panel.

centromeric Rec8 localization at this stage (Fig. 5d). Consistent with this observation, both of these mutant cell types showed precocious centromeric dissociation after meiosis I, and random chromosome segregation following meiosis II (Supplementary Fig. 7). *S. pombe* cells have another PP2A-B56 homologue, Par2, which is expressed at much lower levels[28] and contributes little to centromeric protection in meiosis (data not shown). Taken together, these results argue that, like Sgo1, Sgo1-associating PP2A (including Par1/PP2A-B56) has a crucial role in protecting cohesin at centromeres during meiosis I.

Individual protection ability of PP2A and shugoshin

Our current results in both human cells and fission yeast have raised the possibility that PP2A has an intrinsic ability to protect cohesin. Indeed, by ectopically localizing *S. pombe* Par1/PP2A-B56 to a specific site on a chromosome arm, we observed that the cohesion (and cohesin) at this site was partly preserved even after meiosis I—the period when arm cohesin should dissociate (Supplementary Fig. 8). To assess more thoroughly the individual ability of PP2A for centromeric protection, we used the 'ectopic protection system' in fission yeast, where coexpression of Rec8 and its protector blocks sister chromatid separation in mitosis, causing lethality[8]. We

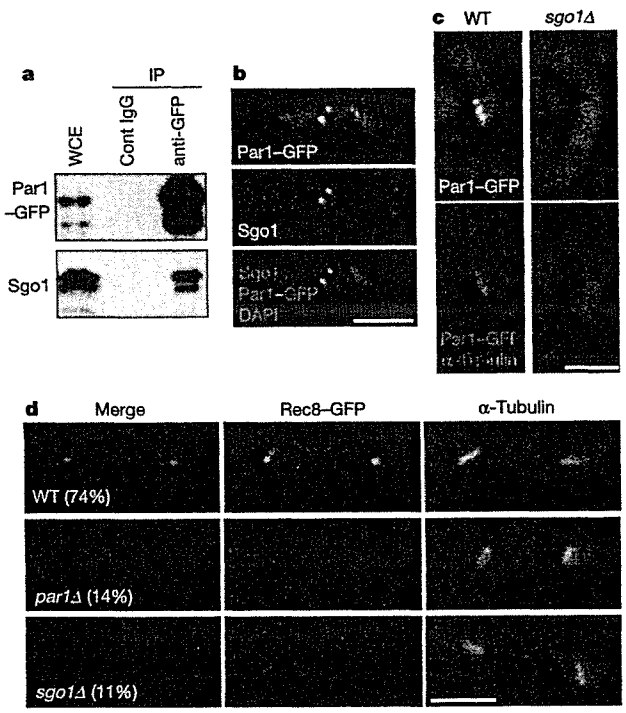

Figure 5 | *S. pombe* PP2A associating with Sgo1 is required for centromeric protection of Rec8-containing cohesin during meiosis I. a, Extracts, prepared from mitotic *par1*$^+$*–GFP* cells ectopically expressing Sgo1, were immunoprecipitated with control IgG or anti-GFP (green fluorescent protein) antibodies and analysed by western blotting using antibodies against GFP and Sgo1. WCE, 7.5% of the whole cell extract. **b,** Meiotic *par1*$^+$*–GFP* cells were arrested at metaphase I by repressing APC activation (*slp1*$^+$ and *cut23*$^+$ expression), and stained with DAPI (4,6-diamidino-2-phenylindole) and antibodies against Sgo1 and GFP. Colocalization was observed in most cells (95%, $n = 20$). **c,** As in **b**, fluorescence of Par1–GFP was examined at metaphase I in wild-type (WT) *sgo1*$^+$ and *sgo1Δ* cells. The spindles were visualized by expressing cyan fluorescent protein (CFP)–Atb2 (α2-tubulin). Par1–GFP was detected as dots in most metaphase I *sgo1*$^+$ cells (98%, $n = 219$), but never in *sgo1Δ* cells (0%, $n = 178$). **d,** The Rec8–GFP signal was monitored at prometaphase II in the indicated strains. Representative samples are shown together with the frequency of the cells showing centromeric Rec8–GFP ($n > 50$).

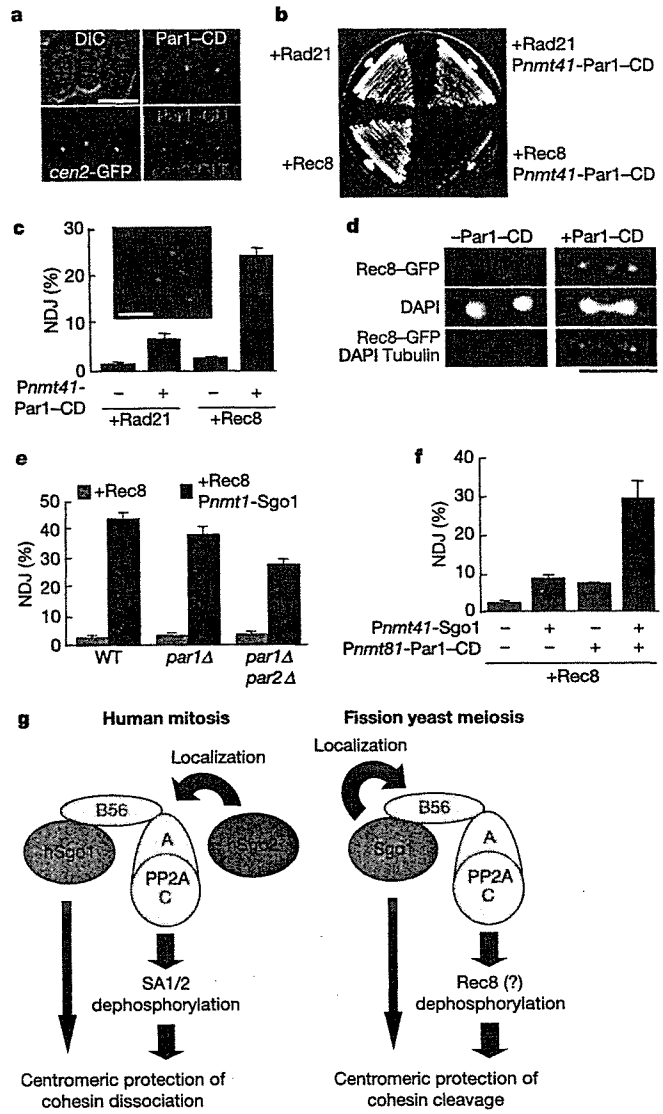

Figure 6 | Individual ability of PP2A and shugoshin for centromeric protection. a, Par1–CD proteins visualized by CFP localized in close vicinity to *cen2*-GFP in proliferating cells. **b,** The haploid *cen2-GFP* strains expressing the indicated genes by exogenous promoters (a constitutive promoter, P*adh1*, for *rad21*$^+$ and *rec8*$^+$, and a thiamine-repressible promoter, P*nmt41*, for *par1*$^+$*–CD*) were streaked on a thiamine-depleted plate. **c,** The strains in **b** were cultured at 30 °C for 15 h after thiamine depletion and the frequency of NDJ was counted among septated cells. Examples of *cen2*-GFP (green) in P*adh1-rec8*$^+$ P*nmt41-par1*$^+$*–CD* cells are shown. **d,** Centromeric Rec8–GFP signals are detected during anaphase in most *par1*$^+$*–CD*-expressing cells (81%) but in fewer non-expressing cells (19%). **e,** The indicated haploid *cen2-GFP* strains expressing Rec8 or Rec8 and Sgo1 (by the P*nmt1* promoter) were examined for the frequency of NDJ among septated cells. **f,** The haploid *cen2-GFP* P*adh1-rec8*$^+$ strains mildly expressing Sgo1 and/or Par1–CD were examined for the frequency of NDJ. Note the different strength of the thiamine repressible promoters (P*nmt1* > P*nmt41* > P*nmt81*). Error bars represent s.d. of triplicate samples (each $n > 100$) (**c**, **e**, **f**). Scale bars, 5 μm (**a**, **c**, **d**). **g,** Model for the collaboration of shugoshin and PP2A in protecting centromeric cohesin during human mitosis and fission yeast meiosis. PP2A containing the B56 subunit, which is recruited to the centromere by shugoshin (hSgo2 in human cells and Sgo1 in *S. pombe*), dephosphorylates cohesin subunits as a mechanism of protection. Human hSgo1 and *S. pombe* Sgo1 may have an individual activity for centromeric protection, apart from localizing PP2A to centromeres.

proposed that PP2A has an intrinsic ability to protect Rec8 without the help of Sgo1 once it is localized to centromeres. To test this, we endowed Par1 with its own ability to localize to centromeres by fusing its C-terminal end with the chromo domain (CD) of Swi6, which binds to Lys-9-methylated histone H3 largely locating at pericentromeric heterochromatin regions—the sites where Sgo1 usually localizes[8]. The engineered protein, Par1–CD, indeed localized at centromeres in mitotic cells in which Sgo1 is not expressed (Fig. 6a). Notably, coexpression of Par1–CD and Rec8 frequently led to blocked nuclear division, as centromere-associated *cen2*-GFP (green fluorescent protein) frequently segregated to the same side of a septated cell (Fig. 6b, c). This non-disjunction (NDJ) of sister chromatids presumably stems from persistent cohesion at anaphase because centromeric cohesin Rec8 was largely protected at this stage (Fig. 6d). Coexpression of Par1–CD with Rad21 caused a much weaker phenotype, indicative of the specificity of protection for the cohesin kleisin subunit (Fig. 6b, c). Finally, the protection is indeed executed by PP2A activity recruited by Par1–CD because the NDJ was suppressed by introducing a mutation in Ppa2, a major catalytic subunit of PP2A in fission yeast[30] (NDJ decreased from 24% to 7%). As Sgo1 is meiosis-specific and is not expressed in mitotic cells, these results demonstrate that centromeric localization of PP2A itself can protect Rec8 cohesin from cleavage, suggesting that dephosphorylation of cohesin Rec8 is a mechanism for the protection of sister centromeres in fission yeast.

We noticed that the ectopic protection mediated by Sgo1 overexpression was alleviated, but not abolished, when endogenous Par1 (or both Par1 and Par2) was depleted from the cells (Fig. 6e). This indicates that Sgo1 also has an individual ability to protect Rec8-containing cohesin without the aid of PP2A-B56 if sufficient amounts of protein are expressed. However, in physiological meiosis, this ability of Sgo1 is not sufficient to complement the loss of PP2A activity. The collaboration of Sgo1 and PP2A was further supported by the observation that coexpression of Sgo1 and Par1–CD mediated a synergistic effect on centromeric protection (Fig. 6f).

Discussion

In animal cells, most cohesin is removed from chromosome arms during prophase and prometaphase, triggered by Plk1-dependent phosphorylation of the Scc3/SA subunit of cohesin[17]. Here we have discovered that a B56-containing subtype of PP2A phosphatase associates with hSgo1 in human cells, playing a crucial part in preventing cohesin dissociation at centromeres. We have also demonstrated that chromatin-bound SA2 at centromeres is mostly dephosphorylated in prometaphase cells, whereas dissociated SA2 from the arms is phosphorylated (Fig. 4a). Furthermore, purified hSgo1 or hSgo2 complex can counteract Plk1-dependent SA phosphorylation *in vitro* (Fig. 4b). Thus, our results argue that dephosphorylation of Scc3/SA by shugoshin-associating PP2A is a mechanism for centromeric protection (Fig. 6g). Because dephosphorylated SA2 is detected only in the chromatin-bound fraction of cohesin, we suggest that the regulation takes place exactly at the sites where shugoshin–PP2A complexes localize. Previous results suggested that Plk-dependent phosphorylation of Scc1/Rad21 facilitates its cleavage by separase but is not essential[17,19,20], whereas phosphorylation of Rec8 might be crucial for cleavage[21,22]. Here we have demonstrated that *S. pombe* Par1/PP2A-B56 associating with Sgo1 is required and even sufficient for protecting cohesin Rec8 from separase cleavage. Moreover, PP2A-dependent cohesin protection requires the kleisin subunit Rec8 (Fig. 6b, c), suggesting that the extent of phosphorylation and/or its contribution to the susceptibility to separase cleavage is different between Scc1/Rad21 and Rec8. These results are consistent with the notion that PP2A activity counteracts the phosphorylation of Rec8, thereby protecting it from separase cleavage during meiosis I. Chromosome segregation in mouse meiosis is also disturbed by okadaic acid treatment, which results in premature separation of sister chromatids during meiosis I[31]. Thus, the shugoshin–PP2A system found in *S. pombe* meiosis is presumably applicable to mammalian meiosis. Taken together, centromeric protection of eukaryotic chromosomes may be executed at the level of dephosphorylation of cohesin subunits, and a subtype of PP2A containing the B56 subunit has a direct role in this process. This concept is applicable for both mitosis and meiosis, albeit the crucial target of dephosphorylation is different, being Scc3/SA in mitosis and Rec8 in meiosis (Fig. 6g).

The depletion of hSgo1 by siRNA caused precocious separation of centromeric cohesion (Fig. 2), although the centromeric localization of PP2A is preserved (Fig. 3c, d), suggesting that protection is not solely executed by linking PP2A to centromeres. Moreover, *hSgo2* siRNA caused fewer defects in protection than *hSgo1* siRNA (Fig. 2e). Therefore, hSgo2 might solely be required to tether PP2A to centromeres, whereas—besides facilitating PP2A function at centromeres—hSgo1 might have an additional role in protection (Fig. 6g). Supporting this notion, ectopic expression of *S. pombe* Sgo1 and Rec8 can enforce centromeric protection even in PP2A-B56-depleted cells (Fig. 6e). Because shugoshin closely associates with cohesin *in vivo*[8,12,32], we favour the possibility that Sgo1 physically protects cohesin against access by an inactivating enzyme (for example, Plk1 in human mitosis and Plk or separase in fission yeast meiosis). As Plk is suggested to phosphorylate and delocalize Sgo/MEI-S332 in *Drosophila*[33], PP2A might facilitate the localization of shugoshin, which is supported by our observation that hSgo1 localization partly depends on PP2A (Fig. 3a). Thus, shugoshin and PP2A may support each other, collaboratively protecting cohesin at centromeres. *S. pombe* Sgo1 has roles in both recruiting PP2A and protecting cohesin *per se* at centromeres. In contrast, hSgo1 is dispensable for localizing PP2A to centromeres but is required for centromeric protection, whereas hSgo2 is required for the recruitment of PP2A to centromeres, implying a 'division of labour' between these two shugoshin-like proteins in human cells. Thus, the interplay of shugoshin and PP2A is apparently conserved across human and fission yeast, or mitosis and meiosis (Fig. 6g).

PP2A is a family of abundantly expressed protein phosphatases, the activity of which is highly regulated and implicated in a multitude of cellular processes, such as signal transduction, development and tumorigenesis[34]. Chromosome mis-segregation in mitosis may contribute to tumorigenesis. Meiotic chromosome segregation is also important clinically, as failures in this process cause birth defects in humans. Our study may provide a novel link between PP2A and tumorigenesis or birth defects, and therefore is useful for future studies in those fields as well.

METHODS

Antibody production and immunofluorescence microscopy. Antibody production and immunofluorescence staining were performed as described in Supplementary Methods.

Quantification of fluorescent signals. To quantify the centromeric fluorescent signals, in-focus images of the cyclin B1-or phospho-H3-positive prometaphase cells were taken with the use of MetaMorph imaging software (Universal Imaging). We measured the maximum intensity among the centromeric signals within the cell and subtracted the background intensity of the region, which was measured directly adjacent to the centromere.

RNA interference. Synthetic sense and antisense siRNA oligonucleotides for *hSgo1* (ref. 14) and *hSgo2* (5′-GCACUACCACUUUGAAUAATT-3′), *PP2A-Aα* (5′-AGACUUGACAUGUUGGUUGTT-3′) and *PP2A-Aβ* (5′-UUUCUACUCC AAGUGCUAGTT-3′) were obtained from JbioS. Note that PP2A-B56 consists of five isoforms, whereas the PP2A-A core subunit has only two isoforms. Therefore, we constructed siRNAs against PP2A-A isoforms, rather than PP2A-B56 isoforms, to reduce PP2A activity. The presented data were obtained using the abovementioned siRNAs, but we confirmed that similar results were obtained by using another set of siRNAs: *hSgo2* (5′-GCUCUCAUGAACAAUAACUTT-3′), *PP2A-Aα* (5′-GCAUCAAUGUGCUGUCUGATT-3′) and *PP2A-Aβ* (5′-CGAC UCAACAGUAUUAAGATT-3′). Cells at 20% confluency in Opti-MEM medium (Invitrogen) were transfected with siRNA duplexes at a final concentration of 400 nM and Oligofectamine (Invitrogen) at 1:250, and complete medium containing 20% FBS was added at 1:1 after 6 h. After two days incubation, the

cells were examined. All control samples were similarly treated but were exposed to H_2O instead of siRNA reagent.

Preparation of HeLa cell extracts. Preparation of HeLa cell extracts and subsequent immunoprecipitation or fractionation are described in Supplementary Methods.

***In vitro* dephosphorylation assay.** To generate phosphorylated SA substrates, a 6× His-tagged SA1 C-terminal peptide (amino acids 923–1258) or SA2 C-terminal peptide (amino acids 895–1232) was expressed in *Escherichia coli* strain BL21 and purified with Ni-NTA agarose (Qiagen), and labelled with [γ-^{32}P]ATP using recombinant Plk1 kinase (ref. 35). As a control, core histone proteins were labelled with [γ-^{32}P]ATP by recombinant Aurora B kinase. The immunoprecipitated complexes from HeLa cell extracts were collected after washing with immunoprecipitation buffer without phosphatase inhibitors (20 mM Tris-HCl, pH 7.5, 100 mM NaCl, 0.1% Tween 20, 10% glycerol and 10 mM β-mercaptoethanol). The equivalent of 3 μl of immunoprecipitated beads was preincubated with 1 μM of okadaic acid or dimethylsulphoxide (DMSO) for 20 min at room temperature (~20 °C), followed by the addition of ^{32}P-labelled SA substrates in a dephosphorylation buffer (50 mM Tris-HCl, pH 7.5, 100 mM NaCl, 0.01% Brij35, 2 mM $MnCl_2$, 0.1 mM EGTA, 2 mM dithiothreitol (DTT)) supplemented with 1 μg of BSA to a total reaction volume of 15 μl and incubated for 2 h at 30 °C with gentle agitation.

Chromosome spreading. Mitotic HeLa cells were collected by mitotic shake-off and treated with 330 nM nocodazole for 4 h. Chromosome spreading was performed as described previously[36].

Yeast experiments. All *S. pombe* strains used are listed in Supplementary Table 1. General methods for immunoprecipitation, culturing *S. pombe*, inducing meiosis and monitoring chromosome segregation were as described previously[8]. Further details of *S. pombe* experiments, as well as the yeast two-hybrid assay, are described in Supplementary Methods.

Received 3 October 2005; accepted 21 February 2006.
Published online 15 March 2006.

1. Nasmyth, K. Disseminating the genome: joining, resolving, and separating sister chromatids during mitosis and meiosis. *Annu. Rev. Genet.* **35**, 673–745 (2001).
2. Milutinovich, M. & Koshland, D. E. SMC complexes–wrapped up in controversy. *Science* **300**, 1101–1102 (2003).
3. Hirano, T. Dynamic molecular linkers of the genome: the first decade of SMC proteins. *Genes Dev.* **19**, 1269–1287 (2005).
4. Hauf, S. & Watanabe, Y. Kinetochore orientation in mitosis and meiosis. *Cell* **119**, 317–327 (2004).
5. Uhlmann, F. Chromosome cohesion and separation: from men and molecules. *Curr. Biol.* **13**, R104–R114 (2003).
6. Lee, J. Y. & Orr-Weaver, T. L. The molecular basis of sister-chromatid cohesion. *Annu. Rev. Cell Dev. Biol.* **17**, 753–777 (2001).
7. Watanabe, Y. Shugoshin: guardian spirit at the centromere. *Curr. Opin. Cell Biol.* **17**, 590–595 (2005).
8. Kitajima, T. S., Kawashima, S. A. & Watanabe, Y. The conserved kinetochore protein shugoshin protects centromeric cohesion during meiosis. *Nature* **427**, 510–517 (2004).
9. Rabitsch, K. P. *et al.* Two fission yeast homologs of *Drosophila Mei-S332* are required for chromosome segregation during meiosis I and II. *Curr. Biol.* **14**, 287–301 (2004).
10. Marston, A. L., Tham, W. H., Shah, H. & Amon, A. A genome-wide screen identifies genes required for centromeric cohesion. *Science* **303**, 1367–1370 (2004).
11. Katis, V. L., Galova, M., Rabitsch, K. P., Gregan, J. & Nasmyth, K. Maintenance of cohesin at centromeres after meiosis I in budding yeast requires a kinetochore-associated protein related to MEI-S332. *Curr. Biol.* **14**, 560–572 (2004).
12. Hamant, O. *et al.* A REC8-dependent plant shugoshin is required for maintenance of centromeric cohesion during meiosis and has no mitotic functions. *Curr. Biol.* **15**, 948–954 (2005).
13. Salic, A., Waters, J. C. & Mitchison, T. J. Vertebrate shugoshin links sister centromere cohesion and kinetochore microtubule stability in mitosis. *Cell* **118**, 567–578 (2004).
14. Kitajima, T. S., Hauf, S., Ohsugi, M., Yamamoto, T. & Watanabe, Y. Human Bub1 defines the persistent cohesion site along the mitotic chromosome by affecting Shugoshin localization. *Curr. Biol.* **15**, 353–359 (2005).
15. McGuinness, B. E., Hirota, T., Kudo, N. R., Peters, J.-M. & Nasmyth, K. Shugoshin prevents dissociation of cohesin from centromeres during mitosis in vertebrate cells. *PLoS Biol.* **3**, e86 (2005).
16. Sumara, I. *et al.* The dissociation of cohesin from chromosomes in prophase is regulated by Polo-like kinase. *Mol. Cell* **9**, 515–525 (2002).
17. Hauf, S. *et al.* Dissociation of cohesin from chromosome arms and loss of arm cohesion during early mitosis depends on phosphorylation of SA2. *PLoS Biol.* **3**, e69 (2005).
18. Losada, A., Hirano, M. & Hirano, T. Cohesin release is required for sister chromatid resolution, but not for condensin-mediated compaction, at the onset of mitosis. *Genes Dev.* **16**, 3004–3016 (2002).
19. Alexandru, G., Uhlmann, F., Mechtler, K., Poupart, M. & Nasmyth, K. Phosphorylation of the cohesin subunit Scc1 by Polo/Cdc5 kinase regulates sister chromatid separation in yeast. *Cell* **105**, 459–472 (2001).
20. Hornig, N. C. & Uhlmann, F. Preferential cleavage of chromatin-bound cohesin after targeted phosphorylation by Polo-like kinase. *EMBO J.* **23**, 3144–3153 (2004).
21. Lee, B. H. & Amon, A. Role of Polo-like kinase *CDC5* in programming meiosis I chromosome segregation. *Science* **300**, 482–486 (2003).
22. Clyne, R. K. *et al.* Polo-like kinase Cdc5 promotes chiasmata formation and cosegregation of sister centromeres at meiosis I. *Nature Cell Biol.* **5**, 480–485 (2003).
23. Natsume, T. *et al.* A direct nanoflow liquid chromatography–tandem mass spectrometry system for interaction proteomics. *Anal. Chem.* **74**, 4725–4733 (2002).
24. Janssens, V. & Goris, J. Protein phosphatase 2A: a highly regulated family of serine/threonine phosphatases implicated in cell growth and signalling. *Biochem. J.* **353**, 417–439 (2001).
25. Tang, Z., Sun, Y., Harley, S. E., Zou, H. & Yu, H. Human Bub1 protects centromeric sister-chromatid cohesion through Shugoshin during mitosis. *Proc. Natl Acad. Sci. USA* **101**, 18012–18017 (2004).
26. Vandre, D. D. & Wills, V. L. Inhibition of mitosis by okadaic acid: possible involvement of a protein phosphatase 2A in the transition from metaphase to anaphase. *J. Cell Sci.* **101**, 79–91 (1992).
27. Van Dolah, F. M. & Ramsdell, J. S. Okadaic acid inhibits a protein phosphatase activity involved in formation of the mitotic spindle of GH4 rat pituitary cells. *J. Cell. Physiol.* **152**, 190–198 (1992).
28. Jiang, W. & Hallberg, R. L. Isolation and characterization of *par1*$^+$ and *par2*$^+$: two *Schizosaccharomyces pombe* genes encoding B′ subunits of protein phosphatase 2A. *Genetics* **154**, 1025–1038 (2000).
29. Le Goff, X. *et al.* The protein phosphatase 2A B′-regulatory subunit par1p is implicated in regulation of the *S. pombe* septation initiation network. *FEBS Lett.* **508**, 136–142 (2001).
30. Kinoshita, N., Ohkura, H. & Yanagida, M. Distinct, essential roles of type 1 and 2A protein phosphatases in control of the fission yeast cell division cycle. *Cell* **63**, 405–415 (1990).
31. Mailhes, J. B., Hilliard, C., Fuseler, J. W. & London, S. N. Okadaic acid, an inhibitor of protein phosphatase 1 and 2A, induces premature separation of sister chromatids during meiosis I and aneuploidy in mouse oocytes *in vitro*. *Chromosome Res.* **11**, 619–631 (2003).
32. Kiburz, B. M. *et al.* The core centromere and Sgo1 establish a 50-kb cohesin-protected domain around centromeres during meiosis I. *Genes Dev.* **19**, 3017–3030 (2005).
33. Clarke, A. S., Tang, T. T., Ooi, D. L. & Orr-Weaver, T. L. POLO kinase regulates the *Drosophila* centromere cohesion protein MEI-S332. *Dev. Cell* **8**, 53–64 (2005).
34. Janssens, V., Goris, J. & Van Hoof, C. PP2A: the expected tumor suppressor. *Curr. Opin. Genet. Dev.* **15**, 34–41 (2005).
35. Nakajima, H., Toyoshima-Morimoto, F., Taniguchi, E. & Nishida, E. Identification of a consensus motif for Plk (Polo-like kinase) phosphorylation reveals Myt1 as a Plk1 substrate. *J. Biol. Chem.* **278**, 25277–25280 (2003).
36. Hauf, S. *et al.* The small molecule Hesperadin reveals a role for Aurora B in correcting kinetochore–microtubule attachment and in maintaining the spindle assembly checkpoint. *J. Cell Biol.* **161**, 281–294 (2003).

Supplementary Information is linked to the online version of the paper at www.nature.com/nature.

Acknowledgements We thank S. Hauf for critically reading the manuscript. We also thank B. Akiyoshi for yeast two-hybrid screening of *S. pombe* Sgo1; K. Nasmyth for communicating unpublished results; J. M. Peters, E. Nishida, F. Ishikawa, Y. Nakatani, M. Sato and T. Toda for reagents; J. M. Peters, M. Ohsugi and M. Shimura for methods; and all members in our laboratory for their valuable discussion and help. K.I. was supported by a JSPS fellowship. This work was supported in part by the New Energy and Industrial Technology Development Organization (to T.N.), and by the Toray Science Foundation, Uehara Memorial Foundation, and a Grant-in-Aid for Specially Promoted Research from the Ministry of Education, Culture, Sports, Science and Technology of Japan (to Y.W.).

Author Contributions Experiments in Figs 1-3 were mainly performed by T.S.K., Fig. 4 by K.I., and Figs 5 and 6 by T.S. and S.A.K. Mass spectrometry of hSgo1 immunoprecipitates was performed by S.I. and T.N. Experimental design, interpretation of data, and the preparation of the manuscript were mainly conducted by T.S.K., T.S., K.I. and Y.W.

Author Information Reprints and permissions information is available at npg.nature.com/reprintsandpermissions. The authors declare no competing financial interests. Correspondence and requests for materials should be addressed to Y.W. (ywatanab@iam.u-tokyo.ac.jp).

MOLECULAR AND CELLULAR BIOLOGY, May 2006, p. 3378–3389
0270-7306/06/$08.00+0 doi:10.1128/MCB.26.9.3378–3389.2006

Vol. 26, No. 9

Cdc37 Interacts with the Glycine-Rich Loop of Hsp90 Client Kinases

Kazuya Terasawa,[1] Katsuhiko Yoshimatsu,[1] Shun-ichiro Iemura,[2] Tohru Natsume,[2] Keiji Tanaka,[3] and Yasufumi Minami[1]*

Department of Biophysics and Biochemistry, and Undergraduate Program for Bioinformatics and Systems Biology, Graduate School of Science, University of Tokyo, Bunkyo-ku, Tokyo 113-0033, Japan[1]; National Institute of Advanced Industrial Science and Technology, Biological Information Research Center, Kohtoh-ku, Tokyo 135-0064, Japan[2]; and Laboratory of Frontier Science, Core Technology and Research Center, Tokyo Metropolitan Institute of Medical Science, Bunkyo-ku, Tokyo 113-8613, Japan[3]

Received 1 December 2005/Returned for modification 19 December 2005/Accepted 10 February 2006

Recently, we identified a client-binding site of Cdc37 that is required for its association with protein kinases. Phage display technology and liquid chromatography-tandem mass spectrometry (which identifies a total of 33 proteins) consistently identify a unique sequence, GXFG, as a Cdc37-interacting motif that occurs in the canonical glycine-rich loop (GXGXXG) of protein kinases, regardless of their dependence on Hsp90 or Cdc37. The glycine-rich motif of Raf-1 (GSGSFG) is necessary for its association with Cdc37; nevertheless, the N lobe of Raf-1 (which includes the GSGSFG motif) on its own cannot interact with Cdc37. Chimeric mutants of Cdk2 and Cdk4, which differ sharply in their affinities toward Cdc37, show that their C-terminal portions may determine this difference. In addition, a nonclient kinase, the catalytic subunit of cyclic AMP-dependent protein kinase, interacts with Cdc37 but only when a threonine residue in the activation segment of its C lobe is unphosphorylated. Thus, although a region in the C termini of protein kinases may be crucial for accomplishing and maintaining their interaction with Cdc37, we conclude that the N-terminal glycine-rich loop of protein kinases is essential for physically associating with Cdc37.

Newly translated proteins must fold correctly into their final conformation in order to perform their given functions, including enzymatic activities and protein-protein interactions among others; however, many proteins are unable to accomplish correct folding by themselves and need the assistance of molecular chaperones (2, 4, 7, 13, 28, 56). Among these chaperones, the 90-kDa heat shock protein, Hsp90, is relatively unique because the proteins that require its assistance (termed Hsp90 client proteins) are apparently limited to cellular signal transducers, such as protein kinases and transcription factors (34–36, 46, 49, 57). Although Hsp90 can bind partially unfolded conformers in the absence of ATP to prevent them from aggregating and to facilitate their (re)folding (6, 25, 26, 52, 55), its in vivo functions essentially depend on ATP binding and hydrolysis (31, 32). Furthermore, the Hsp90 ATPase activity requisite for driving its chaperone cycle is elaborately regulated through sequential and cooperative actions carried out by a constellation of cochaperones (34–36, 46, 49, 57).

Cdc37/p50 is one such Hsp90 cochaperone (14, 23, 33). Recently, it has been shown clearly by crystal structure determination that the N-terminal ATPase domain of Hsp90 associates with the middle segment of Cdc37 (40). Cdc37 appears to be dedicated predominantly to protein kinases (14, 23, 33), which are the largest class of Hsp90 clients (35, 36, 46, 49). Protein kinases are also oncogenic, and their disregulation causes cancers (e.g., ErbB2 [54] and B-Raf [50]). Hsp90 and Cdc37 are overexpressed in malignant cells: their overproduction is induced by oncoproteins that require conformational stabilization because they are fragile, owing to the oncogenic mutations. Consequently, Hsp90 is now an attractive target for the development of new cancer therapeutics (18, 33, 51, 53). One Hsp90 inhibitor, 17-allylaminogeldanamycin, is currently undergoing clinical trials as an antitumor drug; this type of inhibitor competitively occupies the ATP-binding pocket of Hsp90, thereby preventing its chaperone cycle (39, 43). In particular, Hsp90 in tumor cells forms an activated multichaperone complex and is more susceptible to these types of drugs than uncomplexed Hsp90 in normal cells (19). Because these compounds impinge on the Hsp90 molecule, it is assumed that their effects are not restricted to protein kinases but instead will affect the whole range of client proteins. In this regard, it will be necessary to investigate Cdc37 as a possible key component of tumor-specific multichaperone complexes (33).

Although Cdc37 physically interacts with protein kinases (11, 41, 42), this interaction seems to be highly specific. Cdk4, Cdk6, and Cdk7 bind to Cdc37, whereas homologous members of the same family, Cdc2, Cdk2, Cdk3, and Cdk5, do not (3, 20, 44); however, it has recently been reported that Cdk2 is a genuine Hsp90 client kinase (37). Thus, the selective binding of Cdc37 to Hsp90 client kinases may provide a clue for resolving its critical role in the folding of protein kinases assisted by the Hsp90/Cdc37 chaperone machinery. In our recent work, we identified a client-binding site of Cdc37, namely, a 20-residue region (residues 181 to 200) of Cdc37 that can bind Hsp90 client kinases, including Raf-1, Akt1, Aurora B, and Cdk4 (47). Although we found that neither Cdc2 nor Cdk2 bound to full-length Cdc37, consistent with previous studies (20, 44), to our surprise, both proteins associated with an N-terminally

* Corresponding author. Mailing address: Department of Biophysics and Biochemistry, University of Tokyo, Hongo 7-3-1, Bunkyo-ku, Tokyo 133-0033, Japan. Phone and fax: 81-48-268-7274. E-mail: yminami@biochem.s.u-tokyo.ac.jp.

truncated form of Cdc37, composed of residues 181 to 378 [Cdc37(181-378)] that retained the 20-residue region (47).

These puzzling observations have prompted us to determine the Cdc37-interacting region of protein kinases. Using the aforementioned truncated form of Cdc37 as bait, here we have identified a unique sequence (GXFG) as a Cdc37-interacting motif by phage display and liquid chromatography-tandem mass spectrometry (LC-MS/MS) analysis. The sequence is found frequently in the glycine-rich loop (GXGXXG) in the N lobe of protein kinases; this glycine-rich loop is highly conserved among protein kinases, including Hsp90/Cdc37-independent kinases (12, 45). We find that even though the glycine-rich loop of Raf-1 is necessary for its association with Cdc37, neither the N lobe of Raf-1 nor a Raf-1 peptide containing the glycine-rich loop binds to Cdc37. To the contrary, the catalytic subunit of cyclic AMP-dependent protein kinase (PKA), which has been regarded as a nonclient kinase until now (1), interacts with Cdc37 only prior to phosphorylation of the activation segment in its C lobe. In this study, we present evidence that may help to resolve these apparently enigmatic observations and that is crucially required for corroborating our findings; although a region or regions of protein kinases other than the glycine-rich loop, in particular the C-terminal region, may play a significant role in the interaction of these kinases with Cdc37, we demonstrate that the interaction partner of Cdc37 is the canonical glycine-rich loop of protein kinases.

MATERIALS AND METHODS

Plasmid construction. To produce the recombinant protein Cdc37(181-378) fused to glutathione *S*-transferase (GST) [GST-Cdc37(181-378)] in *Escherichia coli*, the BamHI-EcoRI fragment from the construct for Cdc37(181-378) (47) was inserted into a pGEX6P1 plasmid (Amersham Biosciences) that had been cut with both BamHI and EcoRI to yield pGEX6P1-Cdc37(181-378). The preparation of FLAG-tagged Cdc37, Cdc37(1-180), and Cdc37(181-378) [FLAG-Cdc37(181-378), FLAG-Cdc37(1-180), and FLAG-Cdc37(181-378), respectively] has been described previously (47). The plasmids used in this study, pcDL-SRα-456, pcDL-SRα-Myc-GST, SRα-Myc, and pcDNA3FLAG1, and mouse PKA cDNA were supplied by E. Nishida (Kyoto University, Japan). Oligonucleotides containing ATG (for Met), followed by three restriction sites in the order of BglII, EcoRI, and NotI, were introduced into the pcDL-SRα-456 plasmid to obtain pSRα-MCS.

The coding region of enhanced green fluorescent protein (EGFP) was amplified by PCR using a pEGFP-N3 plasmid (Clontech) as a template, with the addition of the oligonucleotide encoding a Myc epitope tag at the 3′ end; the resultant EGFP-Myc fragment was inserted at the NotI site of the pSRα-MCS plasmid to yield pSRα-EGFP-Myc. To obtain constructs for EGFP-fused peptides, oligonucleotides corresponding to peptide sequences were inserted into a pSRα-EGFP-Myc plasmid that had been cut with both BglII and EcoRI. The Myc-tagged and Myc-GST-fused Raf-1 kinase domains have been described previously (47). Constructs for the N lobes of Raf-1 (residues 349 to 423), Cdk2 (residues 1 to 82), and Cdk4 (residues 1 to 95) fused to Myc-tagged GST were produced according to the procedure for the N-terminal portion of Raf-1 (47). To produce a construct for Myc-tagged Cdk2 according to the procedure for Myc-tagged Cdk4 (47), the full-length cDNA of human Cdk2 was synthesized by PCR with reverse transcription using mRNA isolated from HeLa cells, with the addition of a BamHI site at the 5′ end and an EcoRI site following a stop codon (TGA) at the 3′ end.

To obtain cDNAs for chimeric mutants (Cdk2/4 and Cdk4/2), the complementary PCR products for the N-terminal portion of Cdk2 and the C-terminal portion of Cdk4 and those for the reciprocal pair were amplified by PCR. The resulting cDNAs were inserted into a pcDNA3Myc1 plasmid that had been cut with both BamHI and EcoRI; the pcDNA3Myc1 plasmid was made by inserting PCR products containing an oligonucleotide for two copies of Myc epitope flanked by BglII and BamHI-EcoRI sites into pcDNA3 (Invitrogen) that had been double digested with BamHI and EcoRI. Myc-tagged GST fused to the N-terminal portion of the Raf-1 kinase domain (subdomains I to IV) has been described previously (47). The C-terminal portion of the Raf-1 kinase domain (subdomains V to XI) was produced by PCR as described previously (47), and its BamHI/EcoRI fragment was inserted into an SRα-Myc plasmid digested with BglII and EcoRI to produce the Myc-tagged C-terminal portion of the Raf-1 kinase domain. The BamHI fragment of PKA cDNA was inserted into the BamHI site of a pcDNA3Myc1 or pcDNA3FLAG1 plasmid. Mutagenesis of the Raf-1 kinase domain (ASA), its N lobe (ASA), and PKA (TA) was carried out using a QuikChange site-directed mutagenesis kit (Stratagene). All constructs were confirmed by DNA sequencing.

Purification of bacterially expressed recombinant proteins. To obtain the recombinant proteins GST and GST-Cdc37(181-378), the plasmids pGEX6P1 and pGEX6P1-Cdc37(181-378), respectively, were introduced into *E. coli* strain BL21(DE3)pLysS (Stratagene). Cultures were induced with 0.4 mM isopropyl-1-β-D-galactopyranoside after reaching an A_{600} of 0.6 and were further incubated for 1 h at 30°C. Cells were harvested by centrifugation and washed with ice-cold phosphate-buffered saline (137 mM NaCl, 2.68 mM KCl, 8.1 mM Na_2HPO_4, 1.47 mM KH_2PO_4, pH 7.4). The cells were resuspended in phosphate-buffered saline containing 1 mM phenylmethylsulfonyl fluoride and disrupted by sonication; insoluble material was then removed by centrifugation. Recombinant proteins were purified using glutathione Sepharose 4 (Amersham Biosciences) according to the manufacturer's protocol and dialyzed against a buffer solution containing 20 mM Tris-HCl, pH 7.5, 2 mM EGTA, 1 mM dithiothreitol, and 1 mM phenylmethylsulfonyl fluoride.

Phage display technique. A Ph.D.-12 phage display peptide library kit purchased from New England Biolabs was used for affinity panning with GST-Cdc37(181-378). Approximately 1.5×10^{11} phage particles in Tris-buffered saline (TBS; 50 mM Tris-HCl, pH 7.5, 150 mM NaCl) were incubated with GST preadsorbed to glutathione Sepharose 4B for 2 h at 4°C to remove phage particles that were nonspecifically bound to GST, and after clarification by centrifugation, the supernatants were further incubated with GST-Cdc37(181-378)-preadsorbed beads for 2 h. The beads were washed five times with TBS plus 0.1% (vol/vol) Tween 20, and the bound phages were eluted with elution buffer containing 50 mM Tris-HCl, pH 8.0, 2 mM dithiothreitol, and 10 mM reduced glutathione. Recovered phage particles were amplified according to the manufacturer's protocol and affinity panned 3 more times as described above, except that the beads were washed 10 times with TBS plus 0.5% (vol/vol) Tween 20. After the third and fourth rounds of panning, randomly selected phage clones were subjected to DNA sequencing.

Protein identification by LC-MS/MS analysis. FLAG-Cdc37(181-378)-associated complexes were digested with *Achromobacter* protease I, and the resulting peptides were subjected to analysis by a nanoscale LC-MS/MS system (29). The criteria for match acceptance that we used have been reported previously (29).

Cell culture and transfection. COS7 cells were cultured at 37°C in Dulbecco's modified Eagle's medium containing 10% (vol/vol) fetal bovine serum. Cells were transfected with Lipofectamine Plus (Invitrogen), according to the manufacturer's protocol.

Immunoprecipitation and immunoblotting. Cell lysis and immunoprecipitation were carried out essentially as described previously (47). The proteins obtained were separated by sodium dodecyl sulfate-polyacrylamide gel electrophoresis (SDS-PAGE) and analyzed by immunoblotting. Unless otherwise indicated, the anti-Hsp90 antibody used was provided by Y. Miyata (Kyoto University). In the experiment whose results are shown in Fig. 5F, anti-Hsp90 antibody (SPA-830) purchased from Stressgen was used. Anti-Myc (A-14) and anti-Raf-1 (C12) polyclonal antibodies were obtained from Santa Cruz Biotechnology, anti-FLAG polyclonal antibody was obtained from Sigma, anti-Cdc37 polyclonal antibody was obtained from Neomarkers, and PKA C phospho (Thr197) polyclonal antibody was obtained from Cell Signaling.

In vitro binding experiments. FLAG-Cdc37(181-378) and Myc-GST fused to either the kinase domain of Raf-1 or its N lobe were expressed in and purified from COS7 cells as described previously (47). The FLAG-Cdc37(181-378)-adsorbed beads were incubated with 100 μg/ml of FLAG peptide (Sigma) in TBS for 1 h at 4°C to release FLAG-Cdc37(181-378) proteins. The Myc-GST fusion proteins (i.e., the Raf-1 kinase domain and its N lobe) adsorbed to glutathione Sepharose 4B (Amersham Bioscience) were washed with TBS, and then the resin was incubated with the purified FLAG-Cdc37(181-378) proteins in TBS for 2 h at 4°C. The wild-type and ASA mutant forms of Raf-1 peptides (residues 352 to 368), to which six residues of histidine were C terminally added, were purchased from Operon Biotechnologies; briefly, the peptides were synthesized by standard solid phase methods using 9-fluorenylmethoxy carbonyl chemistry and purified by reversed-phase high-performance liquid chromatography. These His-tagged peptides (1 μg) were bound to 10 μl of Ni-NTA agarose (QIAGEN) for 30 min at room temperature, and then the resin was washed with TBS. The recombinant GST-Cdc37(181-378) protein (100 ng) was incubated with the peptide-bound

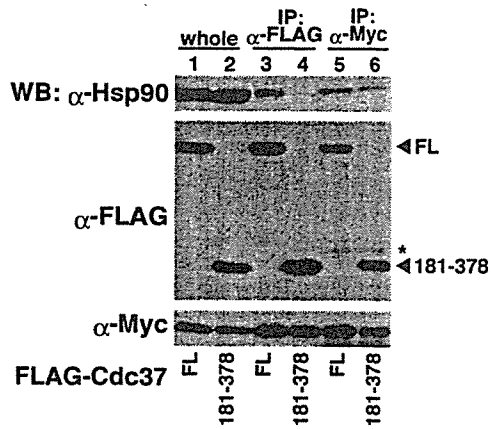

FIG. 1. Cdc37(181-378) interacts directly with the kinase domain of Raf-1. The Myc-tagged kinase domain of Raf-1 and either FLAG-Cdc37 (FL) or FLAG-Cdc37(181-378) (181-378) were expressed in COS7 cells. The cell lysates (whole, lanes 1 and 2) were subjected to immunoprecipitation (IP) with anti-FLAG (IP: α-FLAG, lanes 3 and 4) or anti-Myc (IP: α-Myc, lanes 5 and 6) antibody, followed by immunoblotting (WB) with the indicated antibodies. The asterisk indicates nonspecific bands.

beads in TBS for 2 h at 4°C, and the beads were washed with lysis buffer (20 mM HEPES, pH 7.5, 1 mM $MgCl_2$, 1 mM EGTA, 150 mM NaCl, 1% [vol/vol] Nonidet P-40, and 1% [vol/vol] proteinase inhibitor cocktail [Sigma]).

In vitro translation using rabbit reticulocyte lysate. Using a PKA-inserted pcDNA3FLAG1 plasmid as a template, we amplified by PCR DNA fragments containing the T7 promoter and the PKA-coding regions either with or without a stop codon; the resultant PCR products were used as a template to synthesize PKA mRNAs in the T7 RiboMAX express large-scale RNA production system (Promega) according to the manufacturer's protocol. After purification of the synthesized mRNAs with an RNeasy minikit (QIAGEN), in vitro translation reactions were carried out by using the rabbit reticulocyte lysate system (Promega) for 20 min at 30°C. After protein synthesis, PKA released from the ribosome or the ribosome-bound PKA (corresponding to the DNA construct with or without a stop codon, respectively) was incubated for a further 30 min at 30°C in the presence of 0.2 mg/ml of RNase A (Nippon Gene) to terminate translation or 1 mM puromycin (Sigma) to release translation products from the ribosome, respectively.

Phosphatase treatment. Myc-tagged PKA was immunoprecipitated as described above. The immunoprecipitates were washed with and resuspended in lambda protein phosphatase buffer (New England Biolabs) and then incubated with or without 100 U of lambda protein phosphatase (New England Biolabs) for 45 min at 30°C.

RESULTS

Identification of a Cdc37-interacting motif. Although we have recently identified a client-binding site of Cdc37 that is responsible for its association with Hsp90 client kinases (47), the region or regions in protein kinases that contribute to interaction with Cdc37 remain uncertain. To determine the Cdc37-interacting region in Hsp90 client kinases, we adopted two different experimental approaches (phage display and LC-MS/MS analysis) using a Cdc37(181-378) protein containing the 20-residue client-binding site of Cdc37 as bait; our previous work showed that Cdc37(181-378) binds not only to Hsp90 client kinases (Raf-1, Akt1, Aurora B, and Cdk4) but also to nonclient kinases (Cdc2 and Cdk2) (47).

We examined whether Hsp90 is present in the complex that is formed between Cdc37(181-378) and the kinase domain of Raf-1, albeit Cdc37(181-378) loses the residues involved in its interaction with Hsp90 (i.e., $M^{164}LRR^{167}$ and Asp^{170}) (40). We found that Hsp90 was detected scarcely in the immunoprecipitates of FLAG-tagged Cdc37(181-378), although the Raf-1 kinase domain was efficiently coprecipitated (Fig. 1, lane 4); by contrast, full-length Cdc37 immunoprecipitated Hsp90 together with the Raf-1 kinase domain (Fig. 1, lane 3). In a reciprocal experiment of immunoprecipitation with anti-Myc antibodies (to pull down the Myc-tagged Raf-1 kinase domain), Hsp90 was coprecipitated even in the case of Cdc37(181-378) (Fig. 1, lane 6); however, it is conceivable that this Hsp90 protein interacts directly with the Raf-1 kinase domain that does not associate with Cdc37(181-378). Therefore, we conclude that protein kinases are bound to Cdc37(181-378) directly and not indirectly via Hsp90.

First, we screened a commercially obtained library of random 12-mer peptides fused to a minor coat protein of M13 phage by affinity panning with GST-Cdc37(181-378). After three and four rounds of panning, 11 and 12 clones, respectively, were randomly chosen for DNA sequencing (Table 1). Notably, although peptides of a single sequence or a few specific sequences were not enriched, peptides possessing the sequence GXF (where X is any amino acid) were in the majority (8/11 and 9/12 for the third and fourth rounds of panning, respectively); in addition, most of these peptides had glycine following the phenylalanine (i.e., GXFG).

Next, we attempted to identify proteins that physically interact with Cdc37(181-378) in cells. FLAG-Cdc37(181-378) was expressed in HEK293 cells and immunoprecipitated with anti-FLAG antibody; the immunoprecipitates were digested and then subjected to analysis by a nanoscale LC-MS/MS system (29). A total of 33 proteins met the match acceptance criteria (29) and were specifically identified as interacting with FLAG-Cdc37(181-378) (Table 2). Although two protein kinases (MEKK4 and STE20-like kinase MST4) were identified, it is more intriguing that the sequences GXF and GXY occur in 28 proteins at least once and twice or more in

TABLE 1. Amino acid sequences of randomly selected clones after three and four rounds of affinity panning with GST-Cdc37(181-378)

Sequence type	Sequence after[a]:	
	3rd panning	4th panning
GXFG	TVPHYKIPPGQFg	QLGQPGYFPGSFg
	WYPPYIFPGGGFg	QLGQPGYFPGSFg
	FLPGRFGDEVPW	KQPSYALPQGSFg
	TSLDGDFGRFTL	VGGYNLTPGKFG
	YSIKGSFGPPPT	QLLSGTFGPTYN
	TPRDFQLWSGYFg	STLPAYWLQGSFg
GXF	QYFPGAFASRAN	RTTTDFFPGVFA
	YKMPPGTFQNAS	VGRTFMWTGTFA
		HFVLPPGSFSQS
Other	NKYVVTTPVAFS	TVPLASTPTAPV
	STVAIDPFAPLT	SVSVGMKPSPRP
	EVVKMLLPHVPR	MINSINTVPAPP

[a] The lowercase g indicates the first amino acid of the spacer following the 12-mer peptide.

TABLE 2. Proteins interacting with FLAG-Cdc37(181-378) identified by LC-MS/MS analysis

Protein	No. of occurrences of sequence:	
	GXF (GXFG)	GXY (GXYG)
Acetyl coenzyme A acetyltransferase 1	2 (1)	1 (1)
Cortactin	5 (4)	5 (4)
DEAD box 17	2 (2)	3 (2)
DEAD box 5	2 (1)	2 (0)
DEAD box 3, X linked	4 (1)	6 (2)
DEAD box 3, Y linked	5 (1)	6 (3)
DnaJ homolog, A2	1 (1)	0 (0)
DnaJ homolog, B1	1 (0)	0 (0)
eEF2	2 (0)	2 (1)
eIF4G1	1 (0)	5 (0)
hnRNP A1	5 (4)	6 (3)
hnRNP A2/B1	4 (4)	9 (6)
hnRNP A3	6 (5)	12 (8)
hnRNP M	6 (4)	0 (0)
Hypothetical protein (LOC51244)	2 (0)	0 (0)
Melanoma antigen D1	2 (1)	1 (0)
Melanoma antigen D2	2 (0)	0 (0)
MEKK4	4 (1)	2 (1)
Nup62	4 (0)	0 (0)
Peroxiredoxin 1	2 (0)	1 (0)
Proteasome subunit β7	2 (0)	1 (0)
Rae1	2 (0)	0 (0)
RNA-binding motif protein 14	2 (0)	6 (5)
Ribosomal protein S27	0 (0)	1 (0)
STE20-like kinase MST4	3 (1)	1 (0)
TAR DNA binding protein	5 (4)	0 (0)
Ku antigen	3 (0)	2 (0)
Tim13	1 (1)	0 (0)
ATP synthase γ1	0	0
Dihydrofolate reductase	0	0
NACα	0	0
Tim8	0	0
ZWINT	0	0

most cases; in addition, some of the sequences are followed by glycine (i.e., GXFG and GXYG).

The above-described two experiments afforded us mutually concordant results, that is, Cdc37(181-378) preferably binds a unique sequence, GXF(G). Out of 424 entries of human protein kinases (24), 267 kinases (63%) contain either GXFG (203 kinases) or GXF (64 kinases), and 86 kinases (20%) contain either GXYG (68 kinases) or GXY (18 kinases). Although the sequence GXY(G) was obtained from the pull-down/LC-MS/MS analysis, it was not detected by the phage display, implying that Cdc37(181-378) associates more strongly with GXF(G) than with GXY(G). Importantly, these sequences are located in the so-called glycine-rich loop (GXGXXG), which reportedly helps to anchor the nontransferable phosphates of ATP (12, 45). Furthermore, it is notable that the glycine-rich motif commonly appears in protein kinases regardless of their dependency on Hsp90/Cdc37 (12, 24, 45); thus, even though the glycine-rich motif physically interacts with Cdc37, it cannot be the sole determinant for stable binding of protein kinases to Cdc37.

The glycine-rich loop interacts with Cdc37. The above observations strongly suggest that the glycine-rich loop of protein kinases interacts with Cdc37(181-378). To address this possibility, we examined whether Cdc37(181-378) binds to a Raf-1 peptide containing the Raf-1 glycine-rich loop (Fig. 2A, wt). Immunoprecipitation data indicated that Cdc37(181-378) bound to the Raf-1 peptide conjugated to EGFP-Myc but not to EGFP-Myc alone in COS7 cells (Fig. 2B, compare lanes 5 and 8 with lanes 4 and 7, respectively).

To verify that this interaction was specific and physiologically relevant, we introduced a mutation into Raf-1. A previous study has revealed the significance of the second and third glycines (i.e., Gly^{358} and Gly^{361}, respectively) of the glycine-rich motif of Raf-1 ($G^{356}SGSFG^{361}$) in the interaction of Raf-1 with Cdc37 (58), and furthermore, our above finding suggests that GXFG is preferred by Cdc37; however, when we estimated the phi/psi angles for selected residues (Gly^{358}, Phe^{360}, and Gly^{361}) based on the three-dimensional structure of B-Raf (PDB entry 1UWH [48]), it was suggested that the last glycine (Gly^{361}) is not allowed to be replaced with alanine, although Gly^{358} and Phe^{360} are allowed. Therefore, the glycine-rich motif of Raf-1 was changed to GSASAG to abolish its Cdc37-binding ability (substitutions are underlined). Clearly, the mutant form of the Raf-1 kinase domain did not associate with Cdc37 in COS7 cells (Fig. 2C, ASA), whereas the wild-type Raf-1 kinase domain bound to Cdc37 (Fig. 2C, wt). In addition, the data clearly showed that Cdc37(181-378) bound the Raf-1 kinase domain but did not bind its mutant form (Fig. 2D, compare wt with ASA).

Next, we performed in vitro binding experiments to corroborate the data shown in Fig. 2D; to this end, FLAG-Cdc37(181-378), the Myc-GST-fused Raf-1 kinase domain, and the Myc-GST-fused N lobe of Raf-1 (residues 349 to 423) (45) were expressed in COS7 cells and purified from the cell lysates, as we were not able to bacterially express either the Raf-1 kinase domain or its N lobe in a soluble form (data not shown). A preparation of FLAG-Cdc37(181-378) was highly pure (Fig. 2E, lane 1), and no Hsp90 protein was detected (Fig. 2E, lane 8). Three unknown proteins were invariably present in all preparations of Myc-GST fusion proteins (Fig. 2E, lanes 2 to 6); both wild-type and mutant forms of the N lobe of Raf-1 were substantially pure except for these proteins (Fig. 2E, lanes 3 and 4) and, notably, did not contain Hsp90 (Fig. 2E, lanes 10 and 11). Cdc37(181-378) was pulled down efficiently by the wild-type N lobe of Raf-1, but its ASA mutant lost such an ability (Fig. 2F); thus, the N lobes of Raf-1 and Cdc37(181-378) on their own are sufficient for a stable interaction. As for the kinase domain of Raf-1, we obtained similar results (Fig. 2F): even though, besides its three contaminating bands, a small amount of Hsp90 existed in preparations of both wild-type and mutant forms of the kinase domain (Fig. 2E, lanes 5, 6, 12, and 13), it seems that a physical interaction between Cdc37(181-378) and the kinase domain of Raf-1, which is mediated via the glycine-rich loop and is therefore abrogated by the alanine mutation, was unaffected by this coexisting Hsp90 protein (Fig. 2F).

Finally, the same mutation was introduced into the Raf-1 peptide conjugated to EGFP-Myc (Fig. 2A, ASA); the mutant Raf-1 peptide was profoundly compromised in its ability to associate with Cdc37(181-378) (Fig. 2B, compare lanes 5 and 8 with lanes 6 and 9, respectively). Furthermore, we found that the GST-Cdc37(181-378) recombinant protein (which was used in the phage display) was bound to the His-tagged peptide of the glycine-rich loop of Raf-1 (residues 352 to 368) (Fig. 2A) but that its binding to the ASA mutant peptide was signifi-

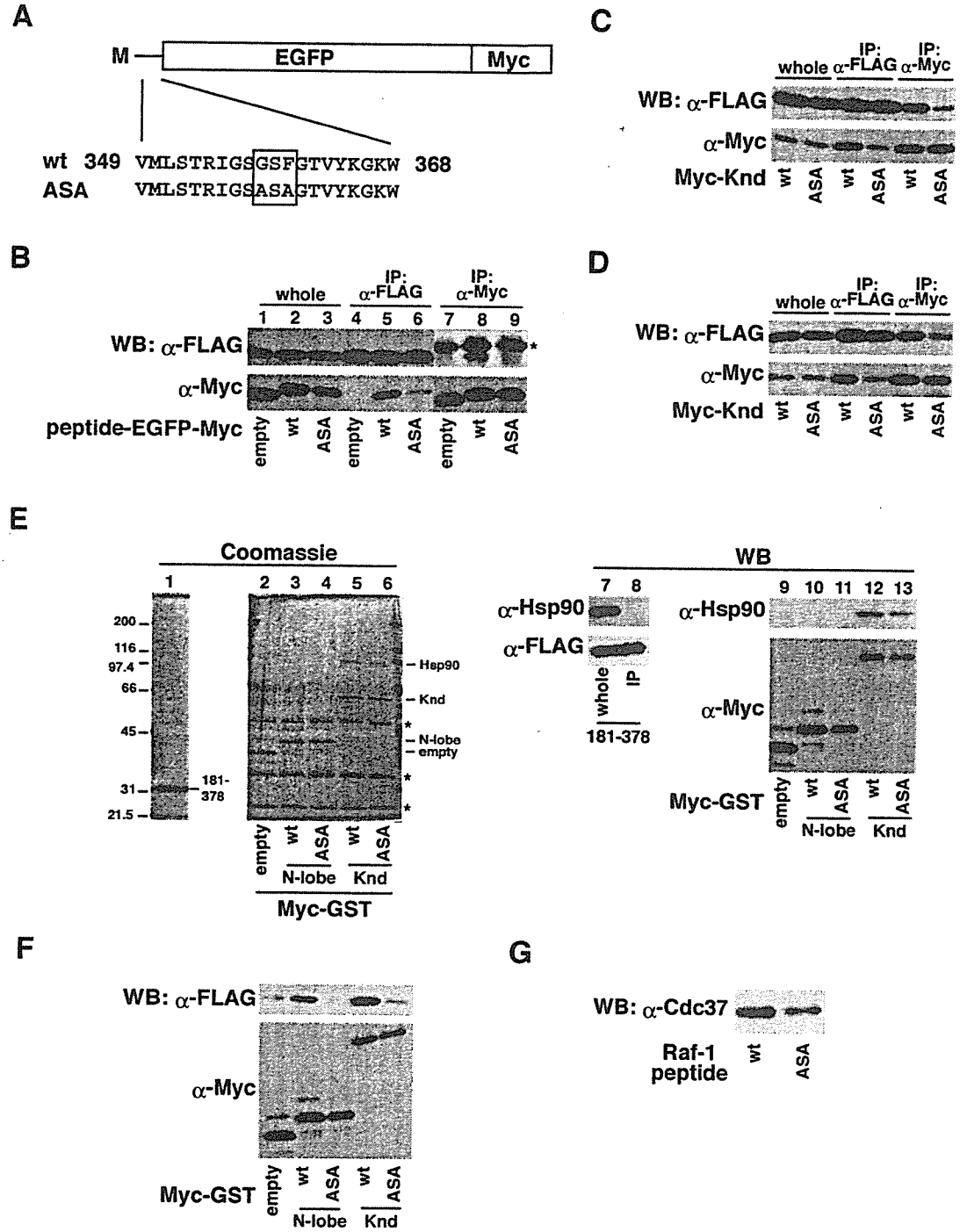

FIG. 2. The glycine-rich loop of Raf-1 interacts with Cdc37. (A) Schematic of the primary structures of the EGFP-Myc fusion proteins showing the peptide sequences of wild-type (wt) and mutant (ASA) Raf-1; the altered amino acids are marked by a box. M indicates the N-terminal methionine. (B) EGFP-Myc alone (empty) and EGFP-Myc fused to the wild-type or mutant Raf-1 peptide were coexpressed with FLAG-Cdc37(181-378) in COS7 cells. Cell extracts (whole, lanes 1 to 3) were subjected to immunoprecipitation with anti-FLAG (IP: α-FLAG, lanes 4 to 6) or anti-Myc (IP: α-Myc, lanes 7 to 9) antibody, followed by immunoblotting with both anti-FLAG and anti-Myc antibodies. The asterisk indicates nonspecific bands. (C and D) Wild-type and mutant forms of the Myc-tagged Raf-1 kinase domain (Myc-Knd) and either FLAG-Cdc37 (C) or FLAG-Cdc37(181-378) (D) were expressed in COS7 cells. The cell lysates (whole) were subjected to immunoprecipitation with anti-FLAG or anti-Myc antibody, followed by immunoblotting with both anti-FLAG and anti-Myc antibodies. (E) FLAG-Cdc37(181-378) (181-378) was expressed in COS7 cells; the cell lysates (whole, lane 7) and purified proteins (IP, lane 8) were immunoblotted with the indicated antibodies. The purified FLAG-Cdc37(181-378) protein was subjected to SDS-PAGE and Coomassie staining (lane 1). Myc-GST (empty) and wild-type (wt) and

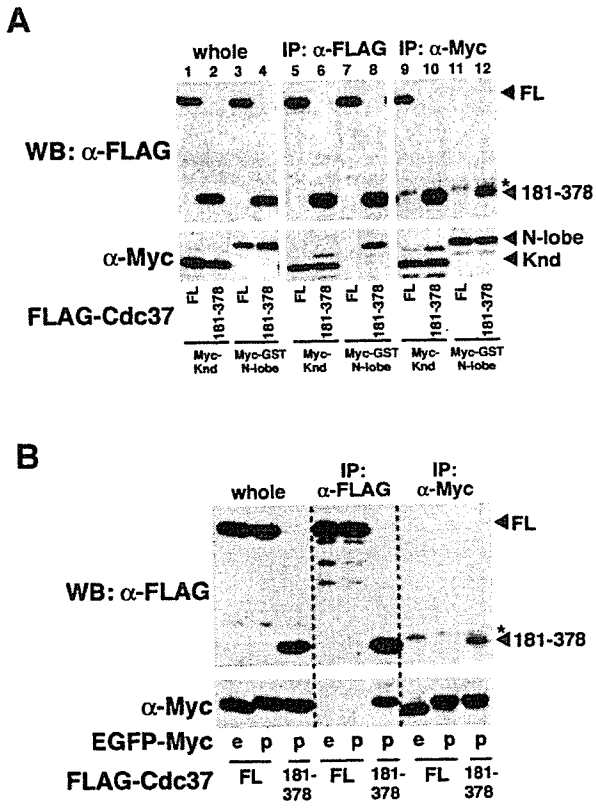

FIG. 3. Full-length Cdc37 does not bind to the N-lobe or glycine-rich loop of Raf-1. (A) Myc-tagged Raf-1 kinase domain (Knd) and Myc-tagged GST fused to the N-lobe of Raf-1 were coexpressed with either FLAG-Cdc37 or FLAG-Cdc37(181-378) (FL or 181-378, respectively) in COS7 cells (whole, lanes 1 to 4), and the indicated immunoprecipitates (IP: α-FLAG, lanes 5 to 8; IP: α-Myc, lanes 9 to 12) were analyzed by immunoblotting with both anti-FLAG and anti-Myc antibodies. (B) FLAG-Cdc37 or FLAG-Cdc37(181-378) was coexpressed in COS7 cells with EGFP-Myc either alone (e) or fused to the Raf-1 peptide (p) shown in Fig. 2A. Cell extracts were prepared (whole) and subjected to immunoprecipitation with anti-FLAG (IP: α-FLAG) or anti-Myc (IP: α-Myc) antibody, followed by immunoblotting as indicated. Asterisks indicates nonspecific bands.

cantly reduced (Fig. 2G). Thus, these data convincingly demonstrate that the glycine-rich loop of Raf-1 is recognized and directly bound by Cdc37(181-378), as predicted from the results obtained by phage display and LC-MS/MS.

Taking these results altogether, we conclude that the glycine-rich loop of protein kinases as well as the client-binding site of Cdc37 (as has been revealed in our previous work [47]) is necessary for the interaction between Cdc37 and protein kinases.

A protein kinase region other than the glycine-rich loop is crucially required for binding to Cdc37. Consistent with the in vitro binding experiments, Cdc37(181-378) was found to bind to the N lobe of Raf-1 fused to Myc-tagged GST in COS7 cells (Fig. 3A, lanes 8 and 12) as well as to its entire kinase domain (Fig. 3A, lanes 6 and 10), whereas Myc-tagged GST alone did not bind to Cdc37(181-378) (data not shown). However, full-length Cdc37 did not interact with the N lobe of Raf-1 (Fig. 3A, lanes 7 and 11), although it bound to the Raf-1 kinase domain (Fig. 3A, lanes 5 and 9). In addition, the Raf-1 peptide containing the glycine-rich loop (Fig. 2A, wt) did not bind to full-length Cdc37 despite its binding to Cdc37(181-378) (Fig. 3B). The fact that full-length Cdc37 can bind neither the N lobe of Raf-1 nor the Raf-1 peptide, both of which contain the glycine-rich loop, seems contradictory to the results presented above. Taken together, these observations seem to indicate that the N lobes of protein kinases alone may be inaccessible to Cdc37, even though they encompasses the Cdc37-interacting region (i.e., the glycine-rich loop); furthermore, it is highly plausible that the residual C lobe may be critically required for the association between Cdc37 and the N lobes of protein kinases.

In this context, it is notable that Cdk2 has been shown to bind to Cdc37(181-378), even though it did not bind to full-length Cdc37 in our previous study (47); on the other hand, its homolog, Cdk4, which is also an Hsp90 client kinase, associates with both Cdc37(181-378) (47) and Cdc37 (3, 20, 44, 47). As shown in Fig. 4A, the N lobes of both Cdk2 and Cdk4 (residues 1 to 82 and 1 to 95, respectively) bound equally well to Cdc37(181-378), in line with the fact that the glycine-rich loops of Cdk2 and Cdk4 have similar sequences (GEGTYG and GVGAYG, respectively).

Thus, we considered that the C lobe of Cdk4 might enable the otherwise incapable N lobe of Cdk2 to interact with Cdc37. Consequently, we generated chimeric mutants of Cdk2 and Cdk4 by swapping their N and C lobes, because these regions are thought to be folded in similar fashions (15, 17). The boundary between the two lobes resides between β-sheet 5 (β5) and α-helix D (αD) (45); however, neither of the two chimeras generated using this boundary associated with Cdc37 (data not shown). As shown in Fig. 4B, the boundary was changed to a more N-terminal position between αC and β4, such that the C-terminal portion corresponded to the C lobe plus two N-terminal β-sheets (β4 and β5). As a result, besides Cdk4 (Fig. 4C, lanes 5 and 9), a Cdk2/4 chimera (Fig. 4C, lanes 6 and 10), in which the N-terminal portion of Cdk2 was joined to the C-terminal portion of Cdk4, was found to interact with

mutant (ASA) forms of Myc-GST fused to either the kinase domain of Raf-1 (Knd) or its N lobe were separated by SDS-PAGE and then subjected to either Coomassie staining (lanes 2 to 6) or immunoblotting with the indicated antibodies (lanes 9 to 13). Asterisks indicate unknown proteins that are present in all preparations of the Myc-GST fusion proteins. Molecular mass markers are shown in kDa on the left of the panel. (F) Myc-GST, the Myc-GST-fused kinase domain of Raf-1, and the Myc-GST-fused N lobe of Raf-1, which were adsorbed to glutathione Sepharose, were incubated with FLAG-Cdc37(181-378) and then subjected to a GST pull-down assay. Samples were analyzed by immunoblotting with the indicated antibodies. (G) Wild-type and mutant forms of the His-tagged Raf-1 peptide adsorbed to Ni-NTA agarose were incubated with recombinant GST-Cdc37(181-378) proteins, and then proteins bound to the peptide-adsorbed resin were analyzed by immunoblotting with anti-Cdc37 antibody.

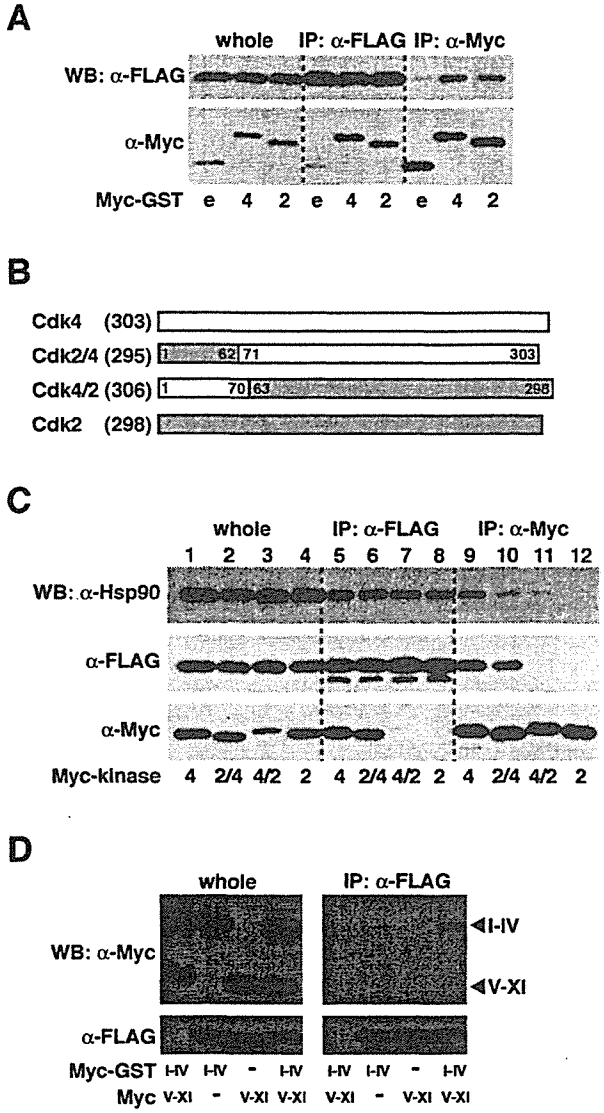

FIG. 4. Chimeric mutants of Cdk2 and Cdk4. (A) FLAG-Cdc37 (181-378) was coexpressed in COS7 cells with Myc-tagged GST (Myc-GST) either alone (e) or fused to the N lobe of Cdk4 or Cdk2 (4 or 2, respectively) and subjected to immunoprecipitation with anti-FLAG (IP: α-FLAG) or anti-Myc (IP: α-Myc) antibody, followed by immunoblotting with anti-FLAG and anti-Myc antibodies. (B) Schematic of Cdk4, Cdk2, and two chimeric mutants. Numbers in parentheses indicate the total number of amino acids; those in boxes indicate the original residue numbers. (C) FLAG-Cdc37 was coexpressed in COS7 cells with the indicated Myc-tagged kinases; Cdk4, Cdk2, and the two chimeric mutants, Cdk2/4 and Cdk4/2, are indicated as 4, 2, 2/4, and 4/2, respectively. Cell extracts (whole, lanes 1 to 4) were subjected to immunoprecipitation (IP: α-FLAG, lanes 5 to 8; IP: α-Myc, lanes 9 to 12) and immunoblotting with anti-Hsp90, anti-FLAG, and anti-Myc antibodies. (D) Myc-GST fused to the N-terminal portion of the Raf-1 kinase domain (I to IV) and/or the Myc-tagged C-terminal portion of the Raf-1 kinase domain (V to XI) was expressed in COS7 cells in the presence or absence of FLAG-Cdc37 as indicated. Cell extracts (whole) were treated as described for panel C.

Cdc37; by contrast, neither a Cdk4/2 chimera (i.e., the inverse of the Cdk2/4 chimera) (Fig. 4C, lanes 7 and 11) nor Cdk2 (Fig. 4C, lanes 8 and 12) associated with Cdc37. Additionally, it seems intriguing that both Cdk4 and Cdk2/4 (Fig. 4C, lanes 9 and 10 [WB: α-Hsp90]) were associated with Hsp90, whereas Cdk2 and Cdk4/2 were not (Fig. 4C, lanes 11 and 12 [WB: α-Hsp90]). By contrast, all immunoprecipitates with anti-FLAG antibody (for the immunoprecipitation of FLAG-tagged Cdc37) contained Hsp90 in comparable amounts (Fig. 4C, lanes 5 to 8 [WB: α-Hsp90]), indicating that Cdc37 directly associates with Hsp90 regardless of its interaction with client kinases.

Taken together, these results suggest that the C-terminal portion (i.e., C lobe plus β4 and β5) of Cdk4 may be responsible for binding of the N-terminal portion, containing the glycine-rich loops of both Cdk2 and Cdk4, to Cdc37, whereas the corresponding C-terminal portion of Cdk2 has no such ability.

Although molecular mechanisms are uncertain at present, we can envisage the following potential scheme: the C-terminal portions of an Hsp90 client kinase (but not a nonclient kinase) directly and/or indirectly (e.g., via interaction with Hsp90, as suggested above) induce conformational alterations in Cdc37 and/or in its N-terminal portions, which in turn enable the N-terminal portion to gain access to Cdc37, thereby facilitating a stable interaction between Cdc37 and the client kinase. To gain more insight into the underlying mechanism, we carried out the following experiment, in which the N- and C-terminal portions of the Raf-1 kinase domain (subdomains I to IV and V to XI, respectively) were coexpressed in cells as separate molecules to explore the ability of the N-terminal portion to interact with Cdc37. Although it has already been shown that the N-terminal (but not the C-terminal) portion of the Raf-1 kinase domain binds to Cdc37(181-378) (47), neither of the regions was able to interact with full-length Cdc37 (Fig. 4D), consistent with the above results (Fig. 3). Of note, the presence of the C-terminal portion of the Raf-1 kinase domain enabled the N-terminal portion to bind to full-length Cdc37 (Fig. 4D). Because the C-terminal portion of the Raf-1 kinase domain was not detected in the resulting complex, the underlying mechanism remains obscure; however, we conclude that the C-terminal portion of the Raf-1 kinase domain can elicit its efficacy toward its N-terminal portion without a molecular linkage between the two regions.

Unphosphorylated PKA binds to Cdc37. We found that PKA did not bind to full-length Cdc37 in cells (Fig. 5A, lanes 4 and 7), indicating that it is a Cdc37-independent kinase, in keeping with a previous study (1). Reminiscent of Cdk2 (Fig. 4), however, PKA associated with Cdc37(181-378) (Fig. 5A, lanes 6 and 9); by contrast, PKA did not interact with Cdc37(1-180), which lacks the client-binding site (Fig. 5A, lanes 5 and 8).

Interestingly, PKA exhibited a doublet band in cells coexpressing Cdc37(181-378) (Fig. 5A, lane 9 [WB: α-Myc]) but not in cells coexpressing full-length Cdc37 and Cdc37(1-180) (Fig. 5A, lanes 7 and 8, respectively [WB: α-Myc]); for unknown reasons, this doublet was undetectable in whole-cell lysates (Fig. 5A, lane 3 [WB: α-Myc]). We considered that the appearance of this doublet might be caused by phosphorylation of PKA, as many protein kinases, including PKA, require phosphorylation of their activation loop to adopt an active confor-

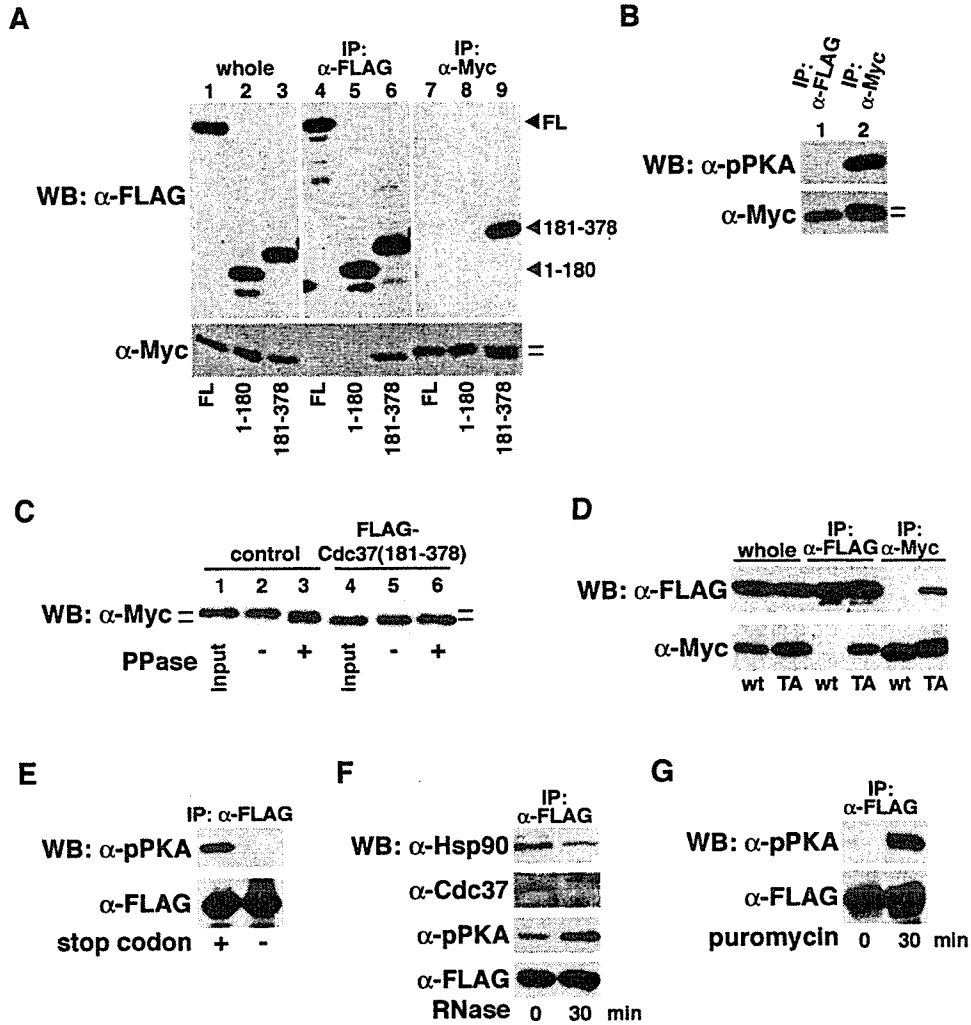

FIG. 5. Unphosphorylated PKA binds to Cdc37. (A) Myc-tagged PKA (Myc-PKA) was coexpressed with FLAG-Cdc37, FLAG-Cdc37(1-180), or FLAG-Cdc37(181-378) in COS7 cells (FL, 1-180, or 181-378, respectively). Cell extracts (whole, lanes 1 to 3) were immunoprecipitated with anti-FLAG (IP: α-FLAG, lanes 4 to 6) or anti-Myc (IP: α-Myc, lanes 7 to 9) antibody and subjected to immunoblotting with both anti-FLAG and anti-Myc antibodies. The two short horizontal lines indicate a doublet band. (B) Myc-PKA and FLAG-Cdc37(181-378) were coexpressed in COS7 cells, and the indicated immunoprecipitates (IP: α-FLAG, lane 1; IP: α-Myc, lane 2) were analyzed by immunoblotting with antiphosphorylated (at Thr^{197}) PKA (α-pPKA) and anti-Myc (to detect Myc-PKA) antibodies. (C) Myc-PKA was expressed in COS7 cells either alone (control, lane 1 to 3) or with FLAG-Cdc37(181-378) [FLAG-Cdc37(181-378), lanes 4 to 6] and purified by immunoprecipitation with anti-Myc or anti-FLAG antibody, respectively. The purified PKA (input, lanes 1 and 4) was either mock treated (without phosphatase [PPase −], lanes 2 and 5) or treated with phosphatase (PPase +, lanes 3 and 6) and subjected to immunoblotting with anti-Myc antibody. (D) Wild-type and mutant forms of Myc-PKA (wt and TA, respectively) were coexpressed with FLAG-Cdc37 in COS7 cells, and the immunoprecipitates obtained were analyzed by immunoblotting with both anti-FLAG and anti-Myc antibodies. (E) FLAG-tagged PKA was translated from mRNAs with or without a stop codon (+ or −, respectively) in rabbit reticulocyte lysate for 20 min at 30°C. Reaction mixtures were immunoprecipitated with anti-FLAG antibody and subjected to immunoblotting with both anti-phosphorylated PKA and anti-FLAG antibodies. (F and G) After protein synthesis, as described for panel E, PKA released from the ribosome (F, RNase at 0 min) or the ribosome-bound PKA (G, puromycin at 0 min) was incubated for a further 30 min at 30°C in the presence of either 0.2 mg/ml of RNase to terminate translation (F, RNase at 30 min) or 1 mM puromycin to release translation products from the ribosome (G, puromycin at 30 min). Immunoprecipitates obtained with anti-FLAG antibody were subjected to immunoblotting with the indicated antibodies.

mation (16, 30). None of the Myc-tagged PKA proteins that coimmunoprecipitated with Cdc37(181-378), as detected by anti-Myc antibody (Fig. 5B, lane 1 [WB: α-Myc]), reacted with antibody specifically recognizing PKA phosphorylated at Thr^{197} of its activation loop (Fig. 5B, lane 1 [WB: α-pPKA]).

The lower band of the doublet seemed to represent the unphosphorylated form of PKA (Fig. 5A, lane 9, and B, lane 2 [WB: α-Myc]), indicating that approximately half of the total amount of PKA was not prevented from being phosphorylated even in the Cdc37(181-378)-expressing cells (Fig. 5B, lane 2). PKA expressed in cells without coexpression of Cdc37(181-378) was completely phosphorylated; therefore, only the upper

band was detected (Fig. 5C, lane 1). By contrast, PKA coexpressed and coimmunoprecipitated with Cdc37(181-378) was unphosphorylated; therefore, only the lower band was visible (Fig. 5C, lane 4). Phosphatase treatment affected only the former type of PKA (Fig. 5C, lanes 2 and 3) and not Cdc37-(181-378)-associated PKA (Fig. 5C, lanes 5 and 6) and resulted in the appearance of the lower unphosphorylated (i.e., dephosphorylated) band (Fig. 5C, lane 3). Taken together, these observations imply that Cdc37(181-378) prevents phosphorylation of PKA by its binding, leading us to assume that even full-length Cdc37 may be able to bind the unphosphorylated form of PKA. To address this issue, Thr^{197} in the activation loop, which must be phosphorylated for activation of PKA (16, 30), was altered to alanine. As expected, the TA mutant form of PKA was strongly bound to Cdc37; however, the wild-type form of PKA was not (Fig. 5D, compare wt with TA). This finding suggests that during the biogenesis of PKA, Cdc37 may bind to PKA in an unphosphorylated state and, on phosphorylation at Thr^{197}, may subsequently dissociate from this kinase.

Consequently, we analyzed whether nascent polypeptide chains of PKA associate with Cdc37 using the reticulocyte lysate system; based on the fact that translation products of mRNAs lacking a stop codon remain ribosome bound as peptidyl-tRNAs (8), PKA was translated using mRNAs either with or without a stop codon. As shown in Fig. 5E, PKA proteins synthesized from mRNA containing a stop codon were phosphorylated, whereas those synthesized from mRNA lacking a stop codon were completely unphosphorylated, implying that phosphorylation occurred post- and not cotranslationally; therefore, completion of translation may be a prerequisite for phosphorylation of PKA at Thr^{197}. To address this issue, translation of PKA (containing a stop codon) was halted by RNase treatment and chased for a further 30 min to examine whether phosphorylation of PKA proteins increased posttranslationally. As expected, phosphorylated PKA significantly increased after 30 min of incubation (Fig. 5F, α-pPKA). Thus, because RNase destroys mRNAs and prevents further initiation/progression of translation, the increase in phosphorylation of PKA must represent posttranslational events. In accord with this idea, ribosome-bound PKA (lacking a stop codon), which was unphosphorylated as shown in Fig. 5E, was efficiently phosphorylated during a chase period after release from the ribosome by puromycin treatment (Fig. 5G). Taken together, these data show that PKA phosphorylation at Thr^{197} is posttranslational and occurs after PKA leaves the ribosome.

Importantly, it was evident that apparently concurrent with PKA phosphorylation, Hsp90 and Cdc37, which associated with PKA before RNase treatment (Fig. 5F, RNase at 0 min), dissociated from PKA (Fig. 5F, RNase at 30 min). Thus, phosphorylation of PKA may induce a conformational alteration that eventually gives rise to the dissociation of Hsp90 and Cdc37, which are probably no longer necessary to maintain PKA folding; alternatively, dissociation of Hsp90 and Cdc37 from PKA may be needed prior to PKA phosphorylation, the mechanism of which is currently unknown. Although PKA has been regarded as a nonclient kinase thus far, our data suggest that its association with Cdc37 (and Hsp90) is required for correct folding during biosynthesis. As such, the standard discrimination between client and nonclient kinases may not be that strict and remains to be reevaluated.

DISCUSSION

Recently, we identified a 20-residue region (residues 181 to 200) of Cdc37 that is necessary for its binding to client protein kinases of Hsp90 and Cdc37 (47). On one hand, by using a series of Cdc37 deletion mutants [especially Cdc37(1-200) and Cdc37(181-378)], it has been revealed that the 20-residue region of Cdc37 is essential for its binding to protein kinases, including Raf-1, Akt1, Aurora B, and Cdk4; to the contrary, neither Cdc37(1-180) nor Cdc37(201-378) associates with Raf-1 (47). On the other hand, others have reported that the N-terminal portion of Cdc37 [Cdc37(1-163) or Cdc37(1-173)] is the substrate-binding domain; however, they did not compare its kinase-binding activity with that of the residual C-terminal region (11, 21). Consequently, we compared the ability of Cdc37(1-163) to bind the Raf-1 kinase domain with that of Cdc37(164-378); as a result, although the N-terminal fragment [Cdc37(1-163)] hardly associated with the kinase domain, the C-terminal fragment [Cdc37(164-378)] exhibited a level of binding activity comparable to those of full-length Cdc37 and Cdc37(181-378) (data not shown). The reason for this discrepancy between our results and those of others remains obscure; notwithstanding, we concluded that Cdc37(181-378) is the minimum region in which the kinase-binding activity is preserved (47), which has been convincingly reinforced in this study. Unexpectedly, however, this N-terminally truncated form of Cdc37, Cdc37(181-378), bound not only Hsp90 client kinases but also nonclient kinases (47).

To resolve these apparently enigmatic observations, here we investigated the regions of protein kinases that bind to Cdc37. Phage display using GST-Cdc37(181-378) as bait successfully afforded us a unique sequence, GXFG, as a candidate for the Cdc37-interacting motif; this motif was reinforced by a pull-down/LC-MS/MS analysis using cells expressing FLAG-Cdc37(181-378), in which many proteins containing GXF(G) and/or GXY(G) were verified to interact with Cdc37(181-378). Interestingly, the sequences GXFG and GXYG are found frequently within a canonical motif of the glycine-rich loop of protein kinases. Using an Hsp90 client kinase, Raf-1, we compellingly demonstrated that Cdc37 physically interacts with the glycine-rich loop of Hsp90 client kinases. However, these results were not seemingly helpful in resolving the initial conundrum, because the glycine-rich loop is common to most protein kinases regardless of whether they are dependent on or independent of Cdc37.

Aside from this issue, the pull-down/LC-MS/MS analysis in the present study fished out various proteins that are functionally divergent besides the two protein kinases, for instance, factors involved in mRNA export (DEAD box RNA helicases, hnRNP proteins, Nup62, and Rae1), factors involved in translation (eEF2, eIF4G1, NACα, and ribosomal protein S27), mitochondrial proteins (acetyl coenzyme A acetyltransferase 1, ATP synthase γ1, Tim8, and Tim13), and DnaJ homologs. It is conceivable that many, but not all, proteins may interact with Cdc37 in the physiological context. Consequently, we focused on the nascent polypeptide-associated complex subunit NACα, as this protein contains neither GXF(G) nor GXY(G); therefore, NACα may associate with Cdc37 in a manner distinct from that of protein kinases. Against expectation, however, no

association between the two proteins in COS7 cells is detected by coimmunoprecipitation experiments (data not shown).

The finding that the interaction partner of Cdc37 is the canonical glycine-rich loop of protein kinases raised the following question: what is the mechanism by which Cdc37 (and Hsp90) makes decisions regarding triage between client and nonclient kinases? Three possibilities, which are not mutually exclusive, may be proposed: first, the glycine-rich loop may be accessible to Cdc37 only in client kinases and not in other kinases; second, most, if not all, protein kinases interact with Cdc37 through the canonical glycine-rich loop at least transiently, but only a select set of them, the "client kinases," maintain this interaction over a longer period; and third, the potential second motif of protein kinases causes a conformational change in Cdc37, thereby exposing its client-binding site or stabilizing its interaction with protein kinases.

Our previous study showed that the Hsp90 client kinase Cdk4 binds to full-length Cdc37 but that its homolog Cdk2 does not, although both of them bind to Cdc37(181-378) (47). The two kinases are considered to have similar architectures (15, 17) and similar sequences in their glycine-rich loops (i.e., GVGAYG for Cdk4 and GEGTYG for Cdk2). Our domain-swapping experiment between these two kinases clearly showed that the C-terminal portion of Cdk4 (in place of the corresponding portion of Cdk2) conferred binding activity on the N-terminal portion of Cdk2, which otherwise could not bind to full-length Cdc37. Thus, as far as Cdk4 is concerned, its C-terminal portion (the C lobe plus β4 and β5) may play a critical role as a determinant for stable binding to Cdc37. Furthermore, full-length Cdc37 did not bind to either the N lobe of Raf-1 or the Raf-1 peptide, both of which contain the glycine-rich loop, which suggests that the C lobe of Raf-1 may contribute significantly to binding of the N lobe to Cdc37. In this regard, it seems noteworthy that the N-terminal portion of the Raf-1 kinase domain (i.e., not exactly the N lobe, but this region lacking only β5) became capable of binding to full-length Cdc37 by coexpression of its C-terminal portion as a separate molecule. It is conceivable that the C-terminal portions of some protein kinases, such as Cdk4 and Raf-1, may be crucially involved in triage decisions regarding whether Hsp90 and Cdc37 are requisite for their correct folding and may ultimately be needed to achieve a stable association with Cdc37 through the glycine-rich loop in their N-terminal portions. Although the molecular mechanisms have not yet been elucidated, the C-terminal portion of protein kinases may behave as an intramolecular chaperone for the N-terminal glycine-rich loop, that is, the C-terminal portion interacts with the glycine-rich loop (or a region containing it) until Cdc37 replaces it. In this regard, it is intriguing that the activation segment in the C lobe of B-Raf possibly associates with its N-terminal glycine-rich loop and that this association is considered to be critical for biogenesis of B-Raf (9, 48), as we will revisit below.

In the present study, we found that the C lobe plus two N-terminal strands (β4 and β5) of Cdk4 were effective in conferring Cdc37-binding activity on the N-terminal portion of Cdk2 but that the C lobe of Cdk4 on its own (i.e., without β4 and β5) had no effect (data not shown). These observations strongly suggest that the boundary region, including the two β-sheets between the two lobes, may significantly contribute to the above-mentioned triage decisions; the boundary separating the two lobes is located between β5 and αD. In this context, a previous study on the tyrosine kinase Lck has suggested that a region between αC and β7 (i.e., αC-β4-β5-αD-αE-β6-β7), which extends across the boundary between the two lobes, is critical for Lck binding to Hsp90 (38).

Although PKA does not reportedly interact with Cdc37, we found that its nonphosphorylated mutant form, in which the phosphorylatable Thr^{197} in the activation loop of its C lobe was replaced with alanine, stably bound to Cdc37. The observation led us to speculate that PKA may not in fact be Cdc37 independent but instead may bind to Cdc37 transiently and dissociate from it immediately upon its phosphorylation at Thr^{197} during biogenesis. Whereas Cdc2 does not physically interact with Cdc37 (20, 44, 47), the yeast Cdc2 homolog Cdc28 has been reported to interact genetically with Cdc37 (5, 10), and a physical interaction between separate domains of Cdc28 and Cdc37 has been shown in a two-hybrid system (27), indicating that Cdc28 (and possibly Cdc2) may physically but temporarily associate with Cdc37, an interaction that is probably undetectable by standard immunoprecipitation techniques. Therefore, not only PKA but also many other protein kinases (probably including Cdc2) that have been regarded as nonclient kinases thus far may not, strictly speaking, be Hsp90/Cdc37-independent kinases; rather, they may associate with Hsp90/Cdc37 during their biogenesis but in an interaction that is relatively transient compared to that with the so-called client kinases.

Our results strongly suggest that dissociation of PKA from Hsp90/Cdc37 occurs concurrently with phosphorylation of its activation loop, although it is uncertain whether dissociation of Hsp90/Cdc37 from PKA causes its phosphorylation or vice versa. Notwithstanding, a close coupling of PKA phosphorylation with Hsp90/Cdc37 dissociation appears convincing and physiologically relevant. In accord with this notion, activation loop autophosphorylation of the dual-specificity tyrosine phosphorylation-regulated protein kinases, which is critical to their maturation, occurs after the completion of translation and has been proposed to be assisted by molecular chaperones (22). B-Raf, which also belongs to the family of Hsp90 client kinases, is mutated at a high frequency in human cancers; in particular, substitution of a glutamate for valine at residue 599 in the activation segment (which includes the activation loop) accounts for more than 90% of the B-Raf mutations (48, 50). In addition, most of the mutations of B-Raf are clustered in the activation segment and in the glycine-rich loop, and the interaction between these two regions is both intimately involved in oncogenesis and critical for its biogenesis (9, 48). Thus, it is possible that Cdc37 (and Hsp90) interacts with B-Raf via its glycine-rich loop and that this interaction is in turn tightly correlated with the intramolecular communication between the glycine-rich loop and the activation segment/loop of B-Raf, as with PKA; however, an investigation from this viewpoint has not yet been done.

In summary, our present study clearly indicates that the C-terminal portions of protein kinases play a crucial role in both accomplishing and maintaining a stable interaction between the glycine-rich loop in the N lobe and Cdc37. Thus, understanding the molecular mechanisms underlying these roles of the C-terminal portions of protein kinases will be necessary to thoroughly delineate the interaction between pro-

tein kinases and Cdc37 in order to provide information that will be essential for the exploitation of Cdc37 as a target for future cancer therapeutics.

ACKNOWLEDGMENTS

We thank E. Nishida, Y. Miyata, and E. Sakai for kindly providing reagents and also thank T. Tanaka for helpful discussion. We also thank members of the Minami lab for their technical assistance and helpful discussion.

This work was supported by grants-in-aid for Scientific Research on Priority Areas and Exploratory Research to Y.M.; Special Coordination Funds for Promoting Science and Technology to K.T. and Y.M. from the Ministry of Education, Culture, Sports, Science and Technology of Japan; and Research on Health Sciences Focusing on Drug Innovation to Y.M. from the Japan Health Sciences Foundation.

REFERENCES

1. **Basso, A. D., D. B. Solit, G. Chiosis, B. Giri, P. Tsichlis, and N. Rosen.** 2002. Akt forms an intracellular complex with heat shock protein 90 (Hsp90) and Cdc37 and is destabilized by inhibitors of Hsp90 function. J. Biol. Chem. **277**:39858–39866.
2. **Bukau, B., E. Deuerling, C. Pfund, and E. A. Craig.** 2000. Getting newly synthesized proteins into shape. Cell **101**:119–122.
3. **Dai, K., R. Kobayashi, and D. Beach.** 1996. Physical interaction of mammalian CDC37 with CDK4. J. Biol. Chem. **271**:22030–22034.
4. **Deuerling, E., and B. Bukau.** 2004. Chaperone-assisted folding of newly synthesized proteins in the cytosol. Crit. Rev. Biochem. Mol. Biol. **39**:261–277.
5. **Farrell, A., and D. Morgan.** 2000. Cdc37 promotes the stability of protein kinases Cdc28 and Cak1. Mol. Cell. Biol. **20**:749–754.
6. **Freeman, B. C., and R. I. Morimoto.** 1996. The human cytosolic molecular chaperone hsp90, hsp70 (hsc70) and hdj-1 have distinct roles in recognition of a non-native protein and protein refolding. EMBO J. **15**:2969–2979.
7. **Frydman, J.** 2001. Folding of newly translated proteins *in vivo*: the role of molecular chaperones. Annu. Rev. Biochem. **70**:603–647.
8. **Frydman, J., E. Nimmesgern, K. Ohtsuka, and F. U. Hartl.** 1994. Folding of nascent polypeptide chains in a high molecular mass assembly with molecular chaperones. Nature **370**:111–117.
9. **Garnett, M. J., and R. Marais.** 2004. Guilty as charged: B-RAF is a human oncogene. Cancer Cell **6**:313–319.
10. **Gerber, M. R., A. Farrell, R. J. Deshaies, I. Herskowitz, and D. O. Morgan.** 1995. Cdc37 is required for association of the protein kinase Cdc28 with G_1 and mitotic cyclins. Proc. Natl. Acad. Sci. USA **92**:4651–4655.
11. **Grammatikakis, N., J.-H. Lin, A. Grammatikakis, P. N. Tsichlis, and B. H. Cochran.** 1999. $p50^{cdc37}$ acting in concert with Hsp90 is required for Raf-1 function. Mol. Cell. Biol. **19**:1661–1672.
12. **Hanks, S. K., and T. Hunter.** 1995. The eukaryotic protein kinase superfamily: kinase (catalytic) domain structure and classification. FASEB J. **9**:576–596.
13. **Hartl, F. U., and M. Hayer-Hartl.** 2002. Molecular chaperones in the cytosol: from nascent chain to folded protein. Science **295**:1852–1858.
14. **Hunter, T., and R. Y. C. Poon.** 1997. Cdc37: a protein kinase chaperone? Trends Cell Biol. **7**:157–161.
15. **Ikuta, M., K. Kamata, K. Fukusawa, T. Honma, T. Machida, H. Hirai, I. Suzuki-Takahashi, T. Hayama, and S. Nishimura.** 2001. Crystallographic approach to identification of cyclin-dependent kinase 4 (CDK4)-specific inhibitors by using CDK4 mimic CDK2 protein. J. Biol. Chem. **276**:27548–27554.
16. **Iyer, G. H., M. J. Moore, and S. S. Taylor.** 2005. Consequences of lysine 72 mutation on the phosphorylation and activation state of cAMP-dependent kinase. J. Biol. Chem. **280**:8800–8807.
17. **Jeffrey, P. D., L. Tong, and N. P. Pavletich.** 2000. Structural basis of inhibition of CDK-cyclin complexes by INK4 inhibitors. Genes Dev. **14**:3115–3125.
18. **Kamal, A., M. F. Boehm, and F. J. Burrows.** 2004. Therapeutic and diagnostic implications of Hsp90 activation. Trends Mol. Med. **10**:283–290.
19. **Kamal, A., L. Thao, J. Sensintaffar, L. Zhang, M. F. Boehm, L. C. Fritz, and F. J. Burrows.** 2003. A high-affinity conformation of Hsp90 confers tumour selectivity on Hsp90 inhibitors. Nature **425**:407–410.
20. **Lamphere, L., F. Fiore, X. Xu, L. Brizuela, S. Keezer, C. Sardet, G. F. Draetta, and J. Gyuris.** 1997. Interaction between Cdc37 and Cdk4 in human cells. Oncogene **14**:1999–2004.
21. **Lee, P., J. Rao, A. Fliss, E. Yang, S. Garrett, and A. J. Caplan.** 2002. The Cdc37 protein kinase-binding domain is sufficient for protein kinase activity and cell viability. J. Cell Biol. **159**:1051–1059.
22. **Lochhead, P. A., G. Sibbet, N. Morrice, and V. Cleghon.** 2005. Activation-loop autophosphorylation is mediated by a novel transitional intermediate form of DYRKs. Cell **121**:925–936.
23. **MacLean, M., and D. Picard.** 2003. Cdc37 goes beyond Hsp90 and kinases. Cell Stress Chaperones **8**:114–119.
24. **Manning, G., D. B. Whyte, R. Martinez, T. Hunter, and S. Sudarsanam.** 2002. The protein kinase complement of the human genome. Science **298**: 1912–1934.
25. **Minami, Y., H. Kawasaki, M. Minami, N. Tanahashi, K. Tanaka, and I. Yahara.** 2000. A critical role for the proteasome activator PA28 in the Hsp90-dependent protein refolding. J. Biol. Chem. **275**:9055–9061.
26. **Miyata, Y., and I. Yahra.** 1992. The 90-kDa heat shock protein, HSP90, binds and protects casein kinase II from self-aggregation and enhances its kinase activity. J. Biol. Chem. **267**:7042–7047.
27. **Mort-Bontemps-Soret, M., C. Facca, and G. Faye.** 2002. Physical interaction of Cdc28 with Cdc37 in *Saccharomyces cerevisiae*. Mol. Genet. Genomics **267**:447–458.
28. **Mosser, D. D., and R. I. Morimoto.** 2004. Molecular chaperones and the stress of oncogenesis. Oncogene **23**:2907–2918.
29. **Natsume, T., Y. Yamauchi, H. Nakayama, T. Shinkawa, M. Yanagida, N. Takahashi, and T. Isobe.** 2002. A direct nanoflow liquid chromatography-tandem mass spectrometry system for interaction proteomics. Anal. Chem. **74**:4725–4733.
30. **Nolen, B., S. Taylor, and G. Ghosh.** 2004. Regulation of protein kinases: controlling activity through activation segment conformation. Mol. Cell **15**: 661–675.
31. **Obermann, W. M. J., H. Sondermann, A. A. Russo, N. P. Pavletich, and F. U. Hartl.** 1998. In vivo function of Hsp90 is dependent on ATP binding and ATP hydrolysis. J. Cell Biol. **143**:901–910.
32. **Panaretou, B., C. Prodromou, S. M. Roe, R. O'Brien, J. E. Ladbury, P. W. Piper, and L. H. Pearl.** 1998. ATP binding and hydrolysis are essential to the function of the Hsp90 molecular chaperone *in vivo*. EMBO J. **17**:4829–4836.
33. **Pearl, L. H.** 2005. Hsp90 and Cdc37—a chaperone cancer conspiracy. Curr. Opin. Genet. Dev. **15**:55–61.
34. **Pearl, L. H., and C. Prodromou.** 2000. Structure and *in vivo* function of Hsp90. Curr. Opin. Struct. Biol. **10**:46–51.
35. **Picard, D.** 2002. Heat-shock protein 90, a chaperone for folding and regulation. Cell. Mol. Life Sci. **59**:1640–1648.
36. **Pratt, W. B., and D. O. Toft.** 2003. Regulation of signaling protein function and trafficking by the hsp90/hsp70-based chaperone machinery. Exp. Biol. Med. **228**:111–133.
37. **Prince, T., L. Sun, and R. L. Matts.** 2005. Cdk2: a genuine protein kinase client of Hsp90 and Cdc37. Biochemistry **44**:15287–15295.
38. **Prince, T., and R. L. Matts.** 2004. Definition of protein kinase sequence motifs that trigger high affinity binding of Hsp90 and Cdc37. J. Biol. Chem. **279**:39975–39981.
39. **Prodromou, C., S. M. Roe, R. O'Brien, J. E. Ladbury, P. W. Piper, and L. H. Pearl.** 1997. Identification and structural characterization of the ATP/ADP-binding site in the Hsp90 molecular chaperone. Cell **90**:65–75.
40. **Roe, S. M., M. M. U. Ali, P. Meyer, C. K. Vaughan, B. Panaretou, P. W. Piper, C. Prodromou, and L. H. Pearl.** 2004. The mechanism of Hsp90 regulation by the protein kinase-specific cochaperone $p50^{cdc37}$. Cell **116**: 87–98.
41. **Shao, J., A. Irwin, S. D. Hartson, and R. L. Matts.** 2003. Functional dissection of Cdc37: characterization of domain structure and amino acid residues critical for protein kinase binding. Biochemistry **42**:12577–12588.
42. **Silverstein, A. M., N. Grammatikakis, B. H. Cochran, M. Chinkers, and W. B. Pratt.** 1998. p50cdc37 binds directly to the catalytic domain of Raf as well as to a site on hsp90 that is topologically adjacent to the tetratricopeptide repeat binding site. J. Biol. Chem. **273**:20090–20095.
43. **Stebbins, C. E., A. A. Russo, C. Schneider, N. Rosen, F. U. Hartl, and N. P. Pavletich.** 1997. Crystal structure of an Hsp90-geldanamycin complex: targeting of a protein chaperone by an antitumor agent. Cell **89**:239–250.
44. **Stepanova, L., X. Leng, S. B. Parker, and J. W. Harper.** 1996. Mammalian $p50^{Cdc37}$ is a protein kinase-targeting subunit of Hsp90 that binds and stabilizes Cdk4. Genes Dev. **10**:1491–1502.
45. **Taylor, S. S., and E. Radzio-Andzelm.** 1994. Three protein kinase structures define a common motif. Structure **2**:345–355.
46. **Terasawa, K., M. Minami, and Y. Minami.** 2005. Constantly updated knowledge of Hsp90. J. Biochem. **137**:443–447.
47. **Terasawa, K., and Y. Minami.** 2005. A client-binding site of Cdc37. FEBS J. **272**:4684–4690.
48. **Wan, P. T. C., M. J. Garnett, S. M. Roe, S. Lee, D. Niculescu-Duvaz, V. M. Good, C. G. Project, C. M. Jones, C. J. Marshall, C. J. Springer, D. Barford, and R. Marais.** 2004. Mechanism of activation of the RAF-ERK signaling pathway by oncogenic mutations of B-RAF. Cell **116**:855–867.
49. **Wegele, H., L. Müller, and J. Buchner.** 2004. Hsp70 and Hsp90—a relay team for protein folding. Rev. Physiol. Biochem. Pharmacol. **151**:1–44.
50. **Wellbrock, C., M. Karasarides, and R. Marais.** 2004. The RAF proteins take centre stage. Nat. Rev. Mol. Cell Biol. **5**:875–885.
51. **Whitesell, L., and S. L. Lindquist.** 2005. Hsp90 and the chaperoning of cancer. Nat. Rev. Cancer **5**:761–772.
52. **Wiech, H., J. Buchner, R. Zimmermann, and U. Jakob.** 1992. Hsp90 chaperones protein folding *in vitro*. Nature **358**:169–170.

53. **Workman, P.** 2004. Combinatorial attack on multistep oncogenesis by inhibiting the Hsp90 molecular chaperone. Cancer Lett. **206**:149–157.
54. **Yarden, Y., and M. X. Sliwkowski.** 2001. Untangling the ErbB signalling network. Nat. Rev. Mol. Cell Biol. **2**:127–137.
55. **Yonehara, M., Y. Minami, Y. Kawata, J. Nagai, and I. Yahara.** 1996. Heat-induced chaperone activity of HSP90. J. Biol. Chem. **271**:2641–2645.
56. **Young, J. C., V. R. Agashe, K. Siegers, and F. U. Hartl.** 2004. Pathways of chaperone-mediated protein folding in the cytosol. Nat. Rev. Mol. Cell Biol. **5**:781–791.
57. **Young, J. C., I. Moarefi, and F. U. Hartl.** 2001. Hsp90: a specialized but essential protein-folding tool. J. Cell Biol. **154**:267–273.
58. **Zhao, Q., F. Boschelli, A. J. Caplan, and K. T. Arndt.** 2004. Identification of a conserved sequence motif that promotes Cdc37 and cyclin D1 binding to Cdk4. J. Biol. Chem. **279**:12560–12564.

THE JOURNAL OF BIOLOGICAL CHEMISTRY VOL. 281, NO. 30, pp. 20749–20760, July 28, 2006

NARF, an Nemo-like Kinase (NLK)-associated Ring Finger Protein Regulates the Ubiquitylation and Degradation of T Cell Factor/Lymphoid Enhancer Factor (TCF/LEF)*[S]

Received for publication, March 6, 2006, and in revised form, May 19, 2006 Published, JBC Papers in Press, May 19, 2006, DOI 10.1074/jbc.M602089200

Misato Yamada[‡1], Junji Ohnishi[‡1], Bisei Ohkawara[‡], Shunichiro Iemura[§], Kiyotoshi Satoh[‡], Junko Hyodo-Miura[¶], Kaoru Kawachi[‡], Tohru Natsume[§], and Hiroshi Shibuya[‡‖2]

From the [‡]Department of Molecular Cell Biology, Medical Research Institute and School of Biomedical Science, Tokyo Medical and Dental University, and SORST, JST, Chiyoda-ku, Tokyo 101-0062, the [‖]Center of Excellence Program for Research on Molecular Destruction and Reconstruction of Tooth and Bone, Tokyo Medical and Dental University, Chiyoda, Tokyo 101-0062, the [§]National Institutes of Advanced Industrial Science and Technology, Biological Information Research Center (JBIRC), Kohtoh-ku, Tokyo 135-0064, and the [¶]Division of Morphogenesis, Department of Developmental Biology, National Institute for Basic Biology, Okazaki 444-8585, Japan

β-Catenin is a key player in the Wnt signaling pathway, and interacts with cofactor T cell factor/lymphoid enhancer factor (TCF/LEF) to generate a transcription activator complex that activates Wnt-induced genes. We previously reported that Nemo-like kinase (NLK) negatively regulates Wnt signaling via phosphorylation of TCF/LEF. To further evaluate the physiological roles of NLK, we performed yeast two-hybrid screening to identify NLK-interacting proteins. From this screen, we isolated a novel RING finger protein that we term NARF (NLK associated RING finger protein). Here, we show that NARF induces the ubiquitylation of TCF/LEF *in vitro* and *in vivo*, and functions as an E3 ubiquitin-ligase that specifically cooperates with the E2 conjugating enzyme E2-25K. We found that NLK augmented NARF binding and ubiquitylation of TCF/LEF, and this required NLK kinase activity. The ubiquitylated TCF/LEF was subsequently degraded by the proteasome. Furthermore, NARF inhibited formation of the secondary axis induced by the ectopic expression of β-catenin in *Xenopus* embryos. Collectively, our findings raise the possibility that NARF functions as a novel ubiquitin-ligase to suppress the Wnt-β-catenin signaling.

The Wnt family of signaling proteins constitutes a large group of highly conserved secreted glycoproteins (1). Wnt proteins are pleiotropic factors that play crucial roles in multiple embryonic developmental processes and also play a role in tumorigenesis (1, 2). Wnt proteins initiate signal transduction via their extracellular surface receptor complex, which is composed of Frizzled proteins (Fz) and lipoprotein receptor-related proteins 5 and 6 (LRP-5/6). In the absence of Wnt stimulation, cytoplasmic β-catenin is maintained at low levels by the continuous process of ubiquitin-proteasome-mediated degradation involving a scaffold complex of axin, adenomatous polyposis coli, (APC) and active glycogen synthasekinase-3β (GSK-3β). In the canonical pathway of β-catenin signal transduction, Wnt signaling relieves this process of proteasome-mediated degradation, and β-catenin consequently accumulates in the cytoplasm. β-Catenin then translocates into the nucleus and forms a transcriptional unit with the HMG box class T cell factor/lymphoid enhancer factor (TCF/LEF)[3] to activate expression of its target genes.

Nemo-like kinase (NLK) was originally isolated as a murine orthologue of the *Drosophila* Nemo by RT-PCR from embryonic mouse brain mRNA using degenerate primers designed for the conserved kinase domains I, VI, VII, and IX of the extracellular-signal regulated kinase/mitogen-activated protein kinase (ERK/MAPK) family (3). The amino acid sequence of the NLK kinase domain shows 39–47% identity to both ERK/MAPK and cyclin-directed kinase 2. The ERK/MAPK family kinases contain a characteristic conserved phosphorylation motif, Thr-*X*-Tyr, in their kinase domain VIII that is required for activation. However, the corresponding sequence in NLK is Thr-Gln-Glu, which is quite similar to the sequence Thr-His-Glu found in some cyclin-directed kinases. The threonine residue in this motif is suggested to be a major site for autophosphorylation of NLK. Thus, NLK may not be a target for an ERK/MAPK activator such as MEK1 (mitogen-activated protein kinase/extracellular signal-regulated kinase kinase) (3).

In our current studies, we demonstrate that NLK is involved in the suppression of the Wnt/β-catenin signaling pathway.

* This work was supported by the Center of Excellence Program for Frontier Research on Molecular Destruction and Reconstruction of Tooth and Bone, a grant-in-aid for scientific research from the Ministry of Education, Science, Sports and Culture of Japan, and grants from The Ichiro Kanehara Foundation, The Naito Foundation, and Yamanouchi Foundation for Research on Metabolic Disorders and Center of Excellence Program for Frontier Research. The costs of publication of this article were defrayed in part by the payment of page charges. This article must therefore be hereby marked "*advertisement*" in accordance with 18 U.S.C. Section 1734 solely to indicate this fact.

[S] The on-line version of this article (available at http://www.jbc.org) contains supplemental Figs. S1 and S2.

[1] Both authors contributed equally to the results of this article.

[2] To whom correspondence should be addressed: Dept. of Molecular Cell Biology, Medical Research Institute, Tokyo Medical and Dental University, Chiyoda, Tokyo 101-0062, Japan. Tel. and Fax: 81-3-5280-8062; E-mail: shibuya.mcb@mri.tmd.ac.jp.

[3] The abbreviations used are: TCF, T cell factor; LEF, lymphoid enhancer factor; NARF, Nemo-like kinase-associated RING finger protein; NLK, Nemo-like kinase; ERK, extracellular signal-regulated kinase; MAPK, mitogen-activated protein kinase; LS-MS/MS, liquid chromatography coupled to tandem mass spectrometry; RT, reverse transcriptase; GST, glutathione *S*-transferase; HA, hemagglutinin; siRNA, small interfering RNA; Ub, ubiquitin.

NLK inactivates a transcriptional unit composed of β-catenin/TCF/LEF via phosphorylation of TCF/LEF, resulting in the inhibition of binding to its target gene sequences (4, 5). NLK functions downstream of transforming growth factor-β-activated kinase 1 (TAK1), a member of the MAPK kinase kinase family (MPAKKK) (4, 6–8), Wnt1 (9), and Wnt5a (10). Our recent data indicate that, in addition to TCF/LEF, NLK associates with and modulates the activities of other transcriptional factors including Sox11 (11), HMG2L1 (12), and STAT3 (6). This suggests that NLK may contribute to various signaling pathways via its ability to interact with a diverse collection of transcription factors.

Alteration in protein function by covalent post-translational modification, including phosphorylation, acetylation, ubiquitylation, sumoylation, neddylation, glycosylation, and ribosylation, is commonly observed in the cell (13–15). Ubiquitylation and phosphorylation are two major types of protein modification and are observed in all eukaryotes. Ubiquitin is a highly conserved 76-amino acid globular protein that can be ligated to proteins and functions to mark them for destruction by the 26 S proteasome (16). In general, ubiquitylation proceeds via a sequential multienzyme reaction directed by E1 ubiquitin-activating enzyme, E2 ubiquitin-conjugating enzyme (also known as Ubc), and E3 ubiquitin-ligase. E1 initiates the first step in the ubiquitylation by forming a thiol-ester bond directly with the carboxyl-terminal glycine of ubiquitin in an ATP-dependent reaction. Subsequently, the activated ubiquitin on E1 is transferred to the cysteine within the active site of an E2 by transesterification. In the last step, E3 associates with ubiquitin-charged E2 and the target protein, and facilitates the formation of an isopeptide linkage between the carboxyl-terminal glycine of ubiquitin and the ε-amino group of an internal lysine residue on the target proteins, or on the extended polyubiquitin chains attached to the protein (17).

Distinctive types of E3 ligases specifically recognize proteins targeted for ubiquitylation. The number of E3 ubiquitin-ligase candidates has vastly expanded to over 100, and these are classified into four major groups based on several motifs: the HECT (homologous to E6-AP carboxyl terminus) domain, the RING (really interesting new gene) finger domain, the U-box, and the PHD (plant homeo-domain) or LAP (leukemia-associate protein) finger domains (15). The RING finger domain in E3 ubiquitin-ligases consists of the conserved sequence motif: C-X_2-C-$X_{(9-39)}$-C-$X_{(1-3)}$-H-$X_{(2-3)}$-C/H-X_2-C-$X_{(4-48)}$-C-X_2-C, and functions to coordinate two zinc ions in a unique "cross-brace" arrangement (18). The family of RING finger proteins can be divided into the single subunit type E3 and the multisubunit type E3. Single subunit type E3 proteins contain the RING finger domain and the substrate recognition site on the same polypeptide. Examples of this type are Mdm2, which ubiquitylates p53 (19, 20), c-Cbl, which ubiquitylates growth factor receptors (21–23), and the inhibitors of apoptosis (24, 25). Multisubunit type E3 proteins contain minimally a small RING finger protein, a member of the cullin family of proteins, and an associated substrate recognition subunit. Well characterized E3 proteins of this type are SCF (25–28) and anaphase-promoting complex (29–31). The SCF ubiquitin-ligase complex contains Skp1, Cul1 (also known as Cdc53), a small RING finger protein Rbx1 (Hrt1/Roc1), and an F-box protein, which provides substrate recognition. Among the substrates ubiquitylated by the SCF complex are β-catenin (32, 33), IκBα (34), and G_1 cyclin (35).

In the present study, we identified a novel RING finger protein that associates with NLK, and termed it NARF (NLK-associating RING finger protein). Biochemical analyses showed that NARF associates with the carboxyl terminus of NLK and provides E3 ubiquitin-ligase activity that specifically cooperates with the E2 ubiquitin-conjugating enzyme E2-25K (Hip-2/UbcH1). We found that NARF targets TCF/LEF proteins for ubiquitylation, and that NLK kinase activity augments this ubiquitylation. NARF-ubiquitylated TCF/LEF is subsequently degraded by the proteasome, resulting in the down-regulation of TCF/LEF-dependent transcriptional activity. In addition to these observations, we found that microinjection of NARF mRNA inhibited secondary axis formation induced by the expression of β-catenin in *Xenopus* embryos. These results reveal a new mechanism for regulating Wnt-β-catenin signaling involving the ubiquitylation and degradation of TCF/LEF proteins by NARF.

EXPERIMENTAL PROCEDURES

Plasmids—The RING finger domain mutants of *Xenopus* NARF at C17A/C53A (xNARF-CA), human NARF at C18A/C54A (hNARF-CA), and a catalytically inactive mutant of *Xenopus* NLK at K89R (xNLK-KN) were generated by site-directed mutagenesis. For generating GST fusion proteins, *Xenopus* NARF wild-type (xNARF-WT) or RING finger domain mutant (xNARF-CA) cDNAs were subcloned into pGEX-4T-1 (Amersham Biosciences). To produce amino-terminal FLAG-tagged or T7-tagged recombinant proteins, cDNAs xNARF-WT, xNARF-CA, human NARF (hNARF-WT), hNARF-CA, xNLK-WT, xNLK-KN, and mouse Wnt1 were subcloned into pCS2 (36). These pCS2-derived plasmids were used to express recombinant proteins in mammalian cells and as templates for *in vitro* transcription to produce RNA for microinjection into *Xenopus* embryos. Amino-terminal hemagglutinin (HA)-tagged or T7-tagged each of xNARF-WT, E2-25K, human TCF4, and human LEF1 were prepared using a mammalian expression vector. FLAG-NLK-ΔN and FLAG-NLK-ΔC were made by deletion of amino acids 1–201 and 202–447 of *Xenopus* NLK, respectively.

Antibodies and Chemicals—The monoclonal antibodies against T7 (Novagen), FLAG (M2, Sigma), HA (16B12, Babco), GST (26H1, Cell Signaling), ubiquitin (P4G7, Covance), TCF4 (6H5-3, Upstate), and β-actin (AC-15, Sigma) were used for immunoprecipitation and/or Western blotting analysis. Anti-NARF rabbit polyclonal antibody was raised against a peptide corresponding to amino acids 234–245 of human NARF, and then affinity purified using antigen-conjugated affinity Sepharose. The proteasome inhibitor MG132 was purchased from Calbiochem.

Yeast Two-hybrid Screening and cDNA Cloning—The yeast two-hybrid screening was performed as previously described (12). A *Xenopus laevis* oocyte MATCHMAKER cDNA library (Clontech) was screened using pGBDU-xNLK-C, which

encodes amino acids 202–447 of *Xenopus* NLK as bait. 3×10^6 clones from a *Xenopus* oocyte cDNA library were screened.

Immunoprecipitation and Western Blotting Analysis—293 cells were cultured at 37 °C in Dulbecco's modified Eagle's medium supplemented with 10% fetal bovine serum. 293 cells (5×10^5 cells) in 60-mm diameter plates were transfected with the indicated plasmids by the calcium phosphate precipitation method. The total amount of plasmids was adjusted to 2.5 μg using the empty expression vector. After 24 h post-transfection, cells were lysed in a buffer containing 50 mM Tris-HCl, pH 7.4, 150 mM NaCl, 5 mM EDTA, 50 mM NaF, 0.5% Nonidet P-40, 1 mM Na_3VO_4, 1 mM phenylmethylsulfonyl fluoride, 1 μg/ml aprotinin, 1 μg/ml pepstatin, 1 μg/ml leupeptin, 1 mM dithiothreitol. Lysates were precleared with protein G-Sepharose beads (Amersham Biosciences) and immunoprecipitated with the appropriate antibodies. To detect the ubiquitylation of TCF/LEF, 293 cells were incubated with 10 μM MG132 for 4 h before harvest and lysed in RIPA buffer containing 10 mM Tris-HCl, pH 7.4, 150 mM NaCl, 5 mM EDTA, 50 mM NaF, 10% glycerol, 1% Triton X-100, 1% sodium deoxycholate, 0.1% SDS, 1 mM phenylmethylsulfonyl fluoride, 1 μg/ml aprotinin, 1 μg/ml pepstatin, 1 μg/ml leupeptin, 1 mM dithiothreitol. Lysates were treated with 1% SDS at 95 °C for 10 min, and diluted 10-fold before use in immunoprecipitation. For Western blotting analysis, whole cell lysates or immunoprecipitates were resolved by SDS-PAGE and transferred to polyvinylidene difluoride membranes (Millipore). The membranes were probed with the appropriate antibody, and proteins of interest were visualized with horseradish peroxidase-conjugated mouse or rabbit IgG using Western Lightning™ Chemiluminescence Reagent *Plus* (PerkinElmer Life Science).

In Vitro Ubiquitylation Assay—Bacterially expressed GST-NARF-WT and GST-NARF-CA were purified with glutathione-Sepharose 4B beads (Amersham Biosciences). For *in vitro* ubiquitylation assays, reactions were performed in 30-μl reaction volumes with the following components as indicated: 0.1 μg of GST-NARF, 0.1 μg of rabbit E1 (Boston Biochem), 0.1 μg of E2-25K (Boston Biochem), 5 μg of ubiquitin (Sigma), 50 mM Tris-HCl, pH 7.4, 0.2 mM ATP, 0.5 mM $MgCl_2$, 0.1 mM dithiothreitol, 1 mM creatine phosphate, 15 units of creatine phosphokinase, and 3 μM ubiquitin aldehyde (Boston Biochem). Reactions were incubated at 30 °C for 2 h and terminated by adding 2× SDS sample buffer and boiled to dissociate proteins. The ubiquitylated proteins were resolved by SDS-PAGE and detected by Western blotting analysis with either anti-ubiquitin antibody (P4G7, Covance) or anti-GST antibody (26H1, Cell Signaling). To detect the ubiquitylation of TCF/LEF *in vitro*, ^{35}S-labeled TCF/LEF was prepared with a TnT-coupled reticulocyte lysate system (Promega) and used as a substrate for the *in vitro* ubiquitylation assay. The ubiquitylated [^{35}S]TCF/LEF was separated by SDS-PAGE and visualized by autoradiography.

Pulse-Chase Assay—293 cells (5×10^5 cells) were transfected with the expression plasmids encoding T7-TCF4, FLAG-NARF, and FLAG-NLK. After 24 h post-transfection, cells were pre-starved for methionine and cysteine for 1 h and labeled for 1 h with 100 μCi/ml Pro-mix L-[^{35}S] *in vitro* cell labeling mixture (Amersham Biosciences). Cells were washed twice and incubated with Dulbecco's modified Eagle's medium containing L-methionine and L-cysteine for the indicated chase periods. At each indicated time point, cells were lysed in RIPA buffer and [^{35}S]T7-tagged TCF4 was immunoprecipitated with anti-T7 antibody (Novagen). Precipitated immune complexes were resolved by SDS-PAGE and ^{35}S-labeled TCF4 was visualized by autoradiography.

RNA Interference—We designed small interference RNAs (siRNAs) against human NARF (sense 5′-GAGAGAGAG-CAUGUCCUGA-3′) mRNA along with its corresponding antisense RNA oligonucleotides with two thymidine residues (dTdT) at the 3′ end of the sequence (Dharmacon). The control siRNA (*siControl*, Dharmacon) is targeted against luciferase. These siRNAs were transfected into 293 cells using Lipofectamine 2000 (Invitrogen). After 24 h post-transfection, cells were used for the experiment.

Semiquantitative Multiplex RT-PCR—Semiquantitative multiplex RT-PCR was performed by the procedure described previously, with some modifications (49). Multiplex PCR was carried out with specific primer sets for human *DKK-1* (sense, 5′-AGG-CGTGCAAATCTGTCTCG-3′; antisense, 5′-TGCATTTGG-ATAGCTGGTTTAGTG-3′) and Quantum RNA classic II 18 S internal standards (Ambion). Aliquots of the PCR products were electrophoresed, visualized with SYBR Green I (Molecular Probes, Inc.), and analyzed by computerized densitometric scanning of the images using Light Capture (ATTO).

Reporter Assay—293 cells (2×10^5 cells) in 35-mm diameter plates were transfected with the indicated plasmids by the calcium phosphate precipitate method. The total amount of plasmids for each transfection was equalized among transfections using empty vector. Cells were harvested after 24 h post-transfection and assayed for luciferase activity.

Secondary Axis Formation—Mature oocytes were collected from *X. laevis* ovaries and *in vitro* fertilization was performed as previously described (50). The jelly layer covering the embryos was removed using 3% cysteine. Capped mRNAs for the indicated proteins were prepared using mMESSAGE mMACHINE SP6 kit (Ambion). Synthesized mRNAs were microinjected into two ventral blastomeres at the 4-cell stage and the ectopic axis formations were counted at tadpole stage.

Protein Identification by LC-MS/MS Analysis—The NARF-associated complexes were digested with *Axhromobacter* protease I, and the resulting peptides were analyzed using a nanoscale LC-MS/MS system as described previously (37).

RESULTS

Identification of NARF as an NLK-associating Protein—To identify protein partners that regulate the signaling of NLK, yeast two-hybrid screening was carried out using the carboxyl terminus encoding amino acids 202–447 of *Xenopus* NLK as bait (11). One of the positive clones was found to encode a novel *Xenopus* sequence containing a characteristic RING finger domain. We termed this protein NARF (accession number DQ011285). Sequence analysis of the full-length NARF cDNA revealed that NARF contains a RING finger domain in the amino terminus and is a *Xenopus* orthologue of a previously uncharacterized human RING finger protein RNF138 (NM 016271), sharing 47% identity (Fig. 1*A*).

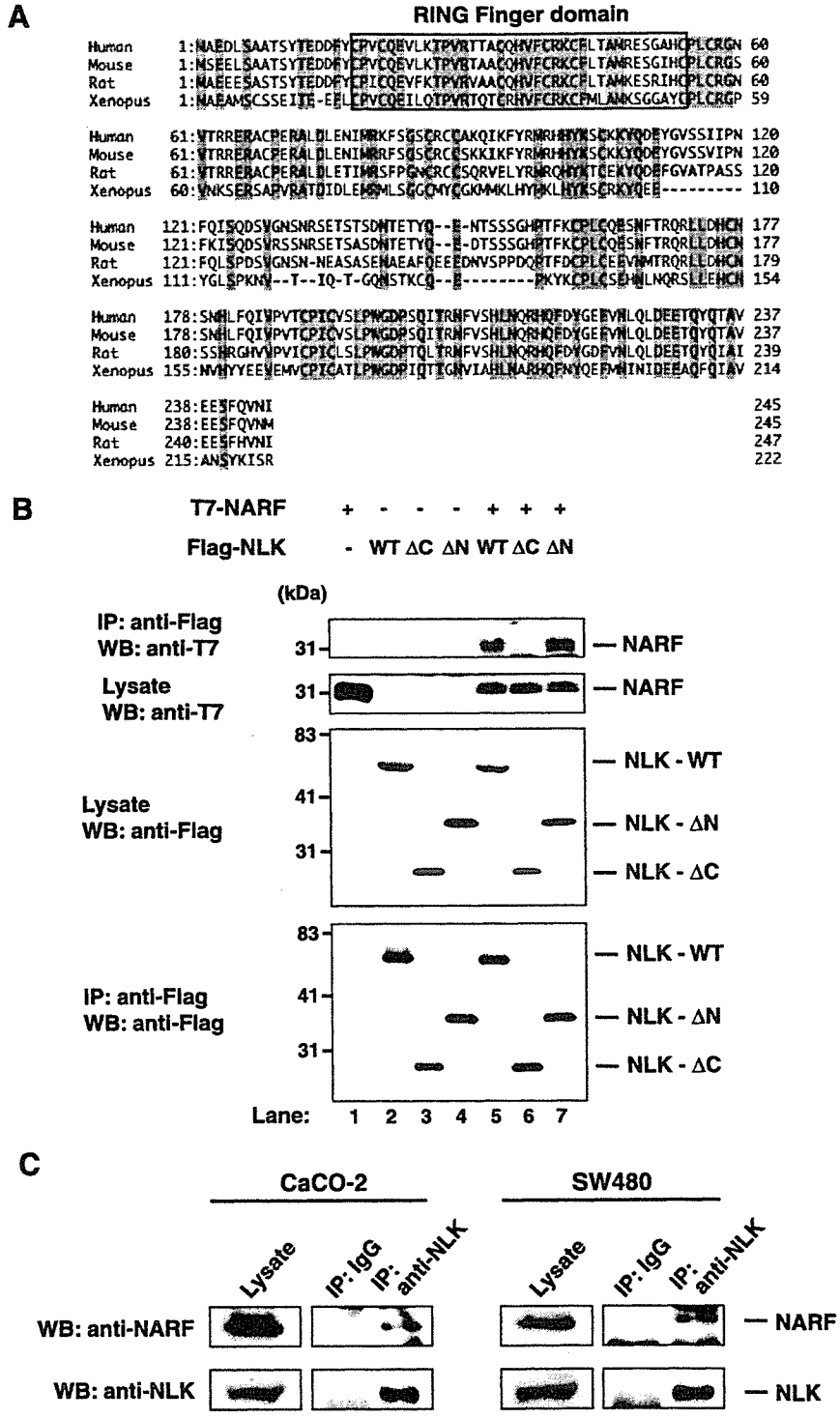

FIGURE 1. **Primary structure of *X. laevis* NARF and association between NARF and NLK.** *A*, *Xenopus* NARF (*xNARF*, accession number DQ011285) and its orthologue from human RING finger protein 138, isoform 1 (*hRNF138*, isoform 1, accession number NP 057355), mouse RNF138, isoform 1 (*mRNF138*, isoform 1, accession number NP 997506), and rat RIKEN cDNA (accession number XP 228926) are shown aligned. Identical residues are *shaded* and the RING finger motif is *boxed*. *B*, 293 cells were transfected with the indicated T7-NARF and FLAG-NLK expression plasmids. *WT*, wild-type NLK; *ΔN*, amino terminus-truncated NLK; *ΔC*, carboxyl terminus-truncated NLK. Immunoprecipitation (*IP*) was carried out with anti-FLAG antibody from whole cell lysates. Co-immunoprecipitation of T7-NARF with FLAG-NLK was visualized by Western blot (*WB*) analysis with anti-T7 antibody (*top panel*). Expression levels of each of the introduced recombinant proteins were apparently equivalent, as judged from Western blotting analysis using whole cell extracts with either anti-T7 antibody for T7-tagged NARF (*second panel*) or anti-FLAG antibody for FLAG-tagged NLKs (*third panel*). Immunoprecipitated FLAG-NLKs were also equivalent (*bottom panel*). *C*, cell lysates were prepared from CaCO-2 and SW480 cells and used for immunoprecipitation with anti-NLK rabbit polyclonal antibody. Rabbit normal IgG was used as control for immunoprecipitation. Co-immunoprecipitation of NARF was visualized by Western blotting with anti-NARF antibody.